revealed loss of full-length plectin with the maintenance of a rodless plectin isoform in EBS-MD. EBS-PA skin specimens harbored greatly reduced amounts of both full-length and rodless plectin.

Protein and mRNA expression patterns of plectin in cultured cells from EBS-MD and EBS-PA patients

Plectin expression patterns of EBS-MD and EBS-PA cultured cells were assessed at both the protein and mRNA levels to confirm the comparative immunofluorescence analysis using skin biopsy specimens showing that the majority of EBS-MD patients expressed a rodless plectin variant, but not full-length plectin and that expression of both full-length and rodless-plectin variant peptides was remarkably reduced or completely abolished in EBS-PA patients. Immunoblot analysis of lysates from fibroblasts of patient EBS-MD5 failed to show any HD1-121 bands, although a band corresponding to rodless plectin was observed by using PN643 and C20 (Fig. 2). Lysates from cultured amniocytes from an aborted sibling of EBS-PA3 (EBS-PA3F) showed that a diminished amount of full-length plectin reacted with PN643, HD1-121, and C20 (Fig. 2).

Using RT-PCR, the presence of an RNA message that does not encode the rod domain was demonstrated in the normal human control as well as the EBS-MD5 and EBS-PA3F cells (Figs. 1C and 5A) (30F/32R). Direct sequencing confirmed the skipping of exon31 in the PCR products (30F/32R) (Fig. 5B). mRNA encoding full-length plectin containing the rod domain was also detected in normal human control, EBS-MD5, and EBS-PA3F cells (Figs. 1C and 5A) (30F/31R and 31F/32R). Judging from the PCR analysis results, the quantity of full-length plectin transcript was greatly reduced in EBS-MD5 and EBS-PA3F compared with those in the normal human controls. In addition, the rodless plectin transcripts were markedly diminished in quantity in EBS-PA3F compared with those of the normal human controls, although expression of the rodless plectin transcripts was maintained in EBS-MD5.

These data suggest that EBS-MD5 fibroblasts express only rodless truncated forms of plectin without the full-length isoform, presumably because of nonsense-mediated mRNA decay (NMD) of the full-length plectin transcript induced by the mutations within *PLEC1* exon 31 (Table 1 and Fig. 1A). Conversely, EBS-PA3F amniocytes expressed a much lower level of plectin than normal human fibroblasts due to NMD of both full-length and rodless plectin transcripts induced by mutations within exons encoding the N-terminal globular domain.

The expression of a small amount of plectin in EBS-PA3 and EBS-PA3F is explained by the splice donor site mutation, c.1344G>A (Table 1 and Fig. 1A). The *PLEC1* cDNA corresponding to exons 9–14 was amplified by PCR using synthesized first-strand cDNA from EBS-PA3F and was cloned into a TA vector. Sequence analysis of the cloned PCR products revealed three different splicing patterns, one of which was a normal transcript from the wild-type allele without c.1344G>A (Fig. 6A and B). In addition to the normal transcript, most of the transcripts derived from the c.1344G>A mutant allele exhibited a 4-bp deletion at nucleotide position 1341–1344 in cDNA (Fig. 6C). This led to a frameshift followed by a PTC at amino acid position 475 (Fig. 6D), whereas small amounts of mRNA exhibiting a

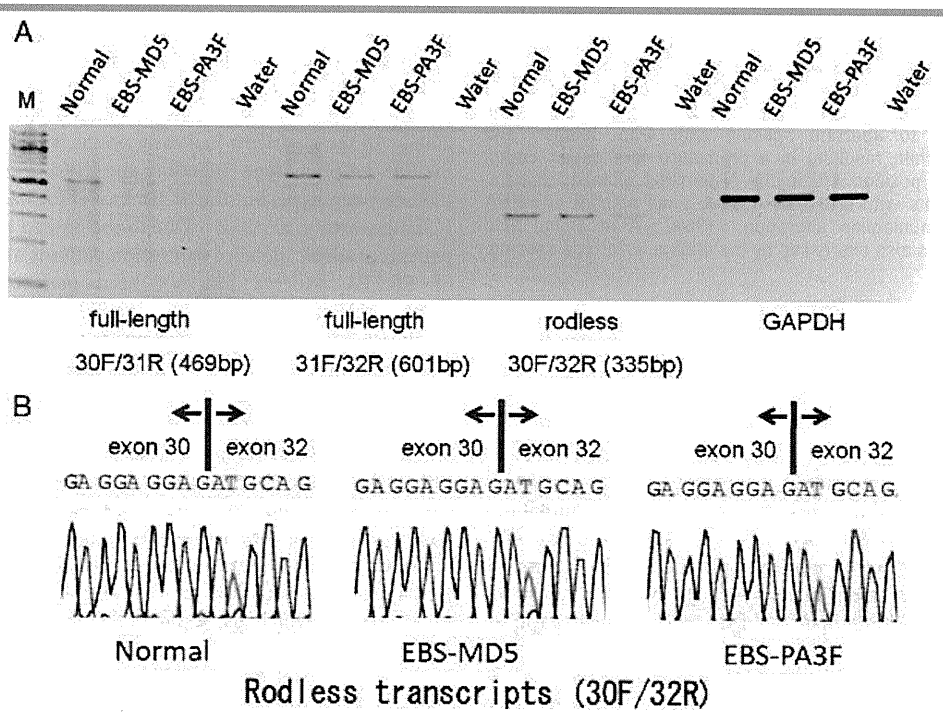

Figure 5. Semiquantitative RT-PCR on full-length and rodless plectin transcripts. **A:** Compared with the normal human control, the EBS-MD5 and EBS-PA3F cells revealed a reduced mRNA level of full-length plectin (30F/31R and 31F/32R). mRNA levels of rodless plectin in EBS-PA3F cells are reduced compared with EBS-MD5 and the normal human control (30F/32R). GAPDH mRNA expression was used as a loading control in these experiments. The negative control reaction (DNA-free water instead of cDNA) shows no PCR products. The molecular weight standard (lane M) is a 100-bp ladder. **B:** Direct sequencing demonstrates skipping of exon 31 in PCR products (30F/32R) from normal human, EBS-MD5, and EBS-PA3F.

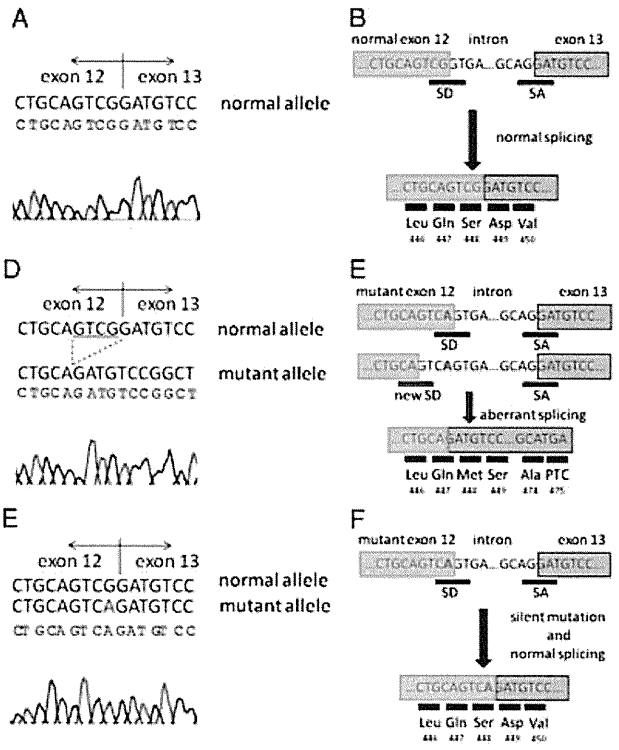

Figure 6. Abnormal splicing due to c.1344G>A mutation in EBS-PA3F, and its consequences **A:** Normal transcripts of the exon 12–exon 13 junction derived from EBS-PA3F cells. **B:** Normal splicing at the exon 12–exon 13 junction. Boxes represent exons, blue underlines are splice sites (SD: splice donor site; SA: splice acceptor site) and black underlined regions are amino acids. **C:** Mutant transcripts with deletion of four nucleotides from exon 12. Deleted nucleotides are underlined. **D:** c.1344G>A mutation altered the G nucleotide of the original splice donor site at the end of exon 12 and activated a cryptic splice donor site (red underline) four nucleotides upstream, leading to aberrant splicing with 4-bp deletion and subsequent frameshift, resulting in a premature termination codon at the amino acid position 475 in the N-terminal globular domain. **E:** Mutant transcripts with c.1344G>A. **F:** A small amount of mRNA carrying a silent nucleotide alteration c.1344G>A at amino acid position 448 Ser was also expressed by the original wild-type splicing.

normal splicing pattern with a silent mutation c.1344G>A at amino acid position 448 Ser were expressed (Fig. 6E and F).

Discussion

This study has demonstrated that two distinct plectin isoforms function in the skin, and that their truncation by *PLEC1* mutations causes the distinct EBS subtypes of EBS-MD and EBS-PA, depending on the pattern of remaining plectin peptide expression.

Plectin has a large rod domain encoded by *PLEC1*exon 31. Alternative splicing of transcripts lacking exon 31 results in a rodless plectin isoform, and it has been demonstrated that the rodless variant is expressed in various rat tissues, including skin, heart, brain, muscle, testis, and liver [Elliott et al., 1997; Fuchs et al., 2005; Steinboeck and Kristufek, 2005]. In addition, the rodless plectin isoform has been found in human muscle cells and keratinocytes [Koster et al., 2004; Schroder et al., 2000]. The significance of this rodless plectin splice variant in the skin remains unclear, but accumulation of *PLEC1* mutational data has revealed that most EBS-MD patients have mutations in exon 31 encoding the large rod domain of plectin, suggesting that conserved expression of the rodless variant plectin could be related to the pathogenesis of EBS-MD in patients with mutations in exon 31 [Pfendner et al., 2005; Sawamura et al., 2007]. However, little data that clarify this hypothesis has been reported, and only one report noted that cultured keratinocytes from one EBS-MD patient were able to express both N- and C-termini plectin epitopes without the expression of rod domain [Koster et al., 2004]. Our data including plectin isoform expression patterns in six EBS-MD patients clearly demonstrate that loss of full-length plectin with conserved rodless plectin isoform expression leads to an EBS-MD phenotype, which is consistent with accumulated clinical and genetic data. We also analyzed the relative amounts of two isoforms of plectin in normal human fibroblasts, keratinocytes, and skeletal muscle (Fig. 3). Our data revealed that the amount of full-length plectin is much greater than that of rodless plectin in fibroblasts and keratinocytes. In contrast, the full-length/rodless ratio in skeletal muscle is a little more than 1. These data are compatible with the fact that EBS-MD patients have skin fragility at birth and develop muscular dystrophy later in life. These data suggests that substantial amounts of rodless plectin in skeletal muscle might delay muscular symptoms while EBS-MD patients are in infancy.

In contrast to the EBS-MD patients, EBS-PA patients are significantly more likely to have mutations in domains outside exon 31 [Pfendner et al., 2005; Sawamura et al., 2007]. The majority of EBS-PA patients included in this study also exhibited *PLEC1* mutations in the gene outside exon 31(Table 1 and Fig. 1A). In the EBS-PA patients in this study, at least one allele is expected to have a stable product (the normal splicing variant from c.1344G>A in EBS-PA1; p.Gln2538X in EBS-PA2, and p.Gln2545X in EBS-PA3). There are three examples in which there are nulls in both alleles that have the PTC outside exon 31 but not in the terminal exon: (1) c.[2727_2740del]+c.[2727_2740del] (exon 22) [Charlesworth et al., 2003], (2) c.[1567_1570del]+c.[1567_1570del] (exon 14) [Pfendner and Uitto, 2005], and (3) p.[Gln305Term]+p.[Gln305Term] (exon 9) [Pfendner and Uitto, 2005]. All three patients had early deaths. Patients (2) and (3) had the EBS-PA phenotype [Pfendner and Uitto, 2005]. Patient (1) had the EBS phenotype, but the occurrence of PA was not substantiated [Charlesworth et al., 2003]. Due to the limited number of EBS-PA patients available, detailed expression patterns of plectin in the skin of EBS-PA patients has not been performed. In addition, comparative analysis of EBS-MD and EBS-PA skin specimens has not been performed. To our knowledge, the present report is the first to compare cutaneous plectin expression in EBS-MD and EBS-PA subtypes using multiple tissues and cells with antibodies that span a range of plectin domains including the N-terminus, rod domain, and C-terminus of plectin. This comparison between EBS-MD and EBS-PA enabled us to identify the differences in these EBS subtypes and to gain a better understanding of the consequences that complete loss or markedly attenuated expression of plectin has. These data are also consistent with the fact that EBS-PA patients generally show more severe skin symptoms than EBS-MD cases, in which expression of a rodless plectin isoform is maintained at least in the skin, although one EBS-PA patient (EBS-PA1) showed a relatively mild skin phenotype [Sawamura et al., 2007]. Also, in some cases of JEB-PA, another subtype of EB with pyloric atresia, the skin manifestations have been reported to be relatively mild and to improve with age, and surgical correction of the PA allowed growth of the patients [Pulkkinen et al., 1998]. It is possible that EBS-PA patients could develop muscular dystrophy if they survived longer. However, to our knowledge, such EBS-PA patients have not been reported in the literature. Figure 7A–C

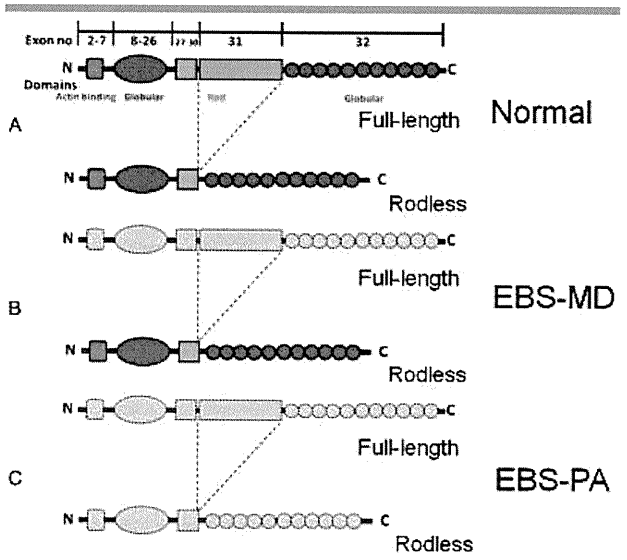

Figure 7. Schematic diagram of cutaneous plectin expression patterns in normal human skin and in skin from EBS-MD and EBS-PA patients. **A:** Two distinct isoforms of plectin—full-length and rodless—are expressed in the normal human control. **B:** Only rodless plectin is expressed in EBS-MD. **C:** Both the full-length and rodless plectin isoforms are greatly diminished or completely lost in EBS-PA. The peptides in light gray are not expressed or are markedly diminished in the patients.

depicts a schematic diagram of the predicted plectin expression pattern among the normal human control, EBS-MD, and EBS-PA.

As described above, almost all EBS-MD patients have one or two truncated mutations in exon 31 encoding the large rod domain of plectin, whereas most *PLEC1* mutations detected in EBS-PA are outside exon 31. To our knowledge, we have three cases of EBS-MD and one case of EBS-PA in the literature whose mutations are not explained by our data: (1) c.[2719_2727del] (exon 21)+c.[2719_2727del] (exon 21) (EBS-MD) [Pulkkinen et al., 1996], (2) c.[1541_1576del] (exon 14)+c.[2677_2685del] (exon 21) (EBS-MD) [Uitto and Pfendner, 2004], (3) c.[2769_2789del] (exon 21)+c.[2769_2789del] (exon 21) (EBS-PA) [Uitto and Pfender, 2005], and (4) c.[13803_13804ins16] (exon 32)+c.[13803_13804ins16] (exon 32) (EBS-MD) [Schroder et al., 2002]. The former three EBS patients had in-frame *PLEC1* deletion mutations outside exon 31 but not in the terminal exon. The last EBS-MD patient was homozygous for out-of-frame mutation in the terminal exon predicting a premature stop-codon within the exon. c.[2719_2727del] was in the nucleotide sequence where CAGGAGGCC was tandemly repeated. Therefore, this in-frame deletion was predicted to result in slipped misparing of DNA [Krawczack and Cooper, 1991; Pfendner and Uitto, 2005]. It is hard to figure out how altered plectin is synthesized from c.[1541_1576del]+c.[2677_2685del] and c.[2769_2789del]+c.[2769_2789del]. It is noteworthy that the phenotype of the EBS-MD patient with c.[1541_1576del]+c.[2677_2685del] was relatively mild, and that muscular dystrophy did not develop until the age of 42 [Uitto and Pfendner, 2004].

In previous studies, the expression of plectin was mainly evaluated by monoclonal antibodies raised against the rod domain. However, several splicing variants had previously prevented us from identifying whether plectin is completely lost or expressed in a truncated protein form in EBS patients with *PLEC1* mutations. Antibodies including those raised against both the plectin N- and C-termini are required to distinguish the expression of rodless splicing variants from a complete protein loss. Nevertheless, we have now elucidated how differences in plectin expression can lead to the two distinct skin blistering-associated phenotypes of muscular dystrophy and pyloric atresia.

Our former study on an EBS-PA3 patient [Nakamura et al., 2005] described different predicted transcripts of the c.1344G>A splice-site mutation from those of the present study. Our previous report employed an exon-trapping system, which is a tool to predict the transcripts that arise from a splice-site mutation when mRNA samples from patient tissues or cells are not available [Buckler et al., 1991]. In that system, the gDNA that is to be screened is subcloned into the exon trapping vector. The subcloned vector is transfected into cells, and mRNA is extracted from the cells to elucidate the splicing consequences. The system is useful, but it is such an artificial way of predicting the splicing products that the induced splicing patterns in the cell culture system are not necessarily correct nor are they the same as those in patient tissues or cultured cells [Schneider et al., 2007]. Because we used cultured amniocytes from EBS-PA3F in the present study, the results shown in Figure 6 supersede the results that were obtained by using an exon-trapping system in the previous report.

To summarize, EBS-MD patients typically express a rodless plectin isoform, although the full-length plectin is lost. In contrast, both full-length and rodless plectin isoforms are deficient in the EBS-PA patients, leading to a more severe disease phenotype. These findings demonstrate that deficiency of both plectin isoforms—full-length and rodless—leads to the severe phenotype of EBS-PA, and in contrast, conserved expression of the rodless isoform results in muscular dystrophy without pyloric atresia. The present results provide important insights toward further understanding the pathomechanisms of muscular dystrophy and pyloric atresia in plectin-deficient patients.

Acknowledgments

We thank Dr. G. Wiche for providing mAb 5B3 and 10F6 and Ms. Yuko Hayakawa for her technical assistance. This work was supported by Health and Labor Sciences Research grants for Research on Measures for Intractable Diseases, from the Ministry of Health, Labor, and Welfare of Japan; by the German EB-Network grant from the Ministry for Education and Research; and by the Excellence Initiative of the German Federal and State Governments (Freiburg Institute for Advanced Studies, FRIAS, School of Life Sciences).

References

Bauer JW, Rouan F, Kofler B, Rezniczek GA, Kornacker I, Muss W, Hametner R, Klausegger A, Huber A, Pohla-Gubo G, Wiche G, Uitto J, Hintner H. 2001. A compound heterozygous one amino-acid insertion/nonsense mutation in the plectin gene causes epidermolysis bullosa simplex with plectin deficiency. Am J Pathol 158:617–625.

Boczonadi V, McInroy L, Maatta A. 2007. Cytolinker cross-talk: periplakin N-terminus interacts with plectin to regulate keratin organisation and epithelial migration. Exp Cell Res 313:3579–3591.

Borradori L, Sonnenberg A. 1999. Structure and function of hemidesmosomes: more than simple adhesion complexes. J Invest Dermatol 112:411–418.

Buckler AJ, Chang DD, Graw SL, Brook JD, Haber DA, Sharp PA, Housman DE. 1991. Exon amplification: a strategy to isolate mammalian genes based on RNA splicing. Proc Natl Acad Sci USA 88:4005–4009.

Charlesworth A, Gagnoux-Palacios L, Bonduelle M, Ortonne JP, De Raeve L, Meneguzzi G. 2003. Identification of a lethal form of epidermolysis bullosa simplex associated with a homozygous genetic mutation in plectin. J Invest Dermatol 121:1344–1348.

Chavanas S, Pulkkinen L, Gache Y, Smith FJ, McLean WH, Uitto J, Ortonne JP, Meneguzzi G. 1996. A homozygous nonsense mutation in the PLEC1 gene in patients with epidermolysis bullosa simplex with muscular dystrophy. J Clin Invest 98:2196–2200.

Dang M, Pulkkinen L, Smith FJ, McLean WH, Uitto J. 1998. Novel compound heterozygous mutations in the plectin gene in epidermolysis bullosa with

muscular dystrophy and the use of protein truncation test for detection of premature termination codon mutations. Lab Invest 78:195–204.
Elliott CE, Becker B, Oehler S, Castanon MJ, Hauptmann R, Wiche G. 1997. Plectin transcript diversity: identification and tissue distribution of variants with distinct first coding exons and rodless isoforms. Genomics 42:115–125.
Fine JD, Eady RA, Bauer EA, Bauer JW, Bruckner-Tuderman L, Heagerty A, Hintner H, Hovnanian A, Jonkman MF, Leigh I, McGrath JA, Mellerio JE, Murrell DF, Shimizu H, Uitto J, Vahlquist A, Woodley D, Zambruno G. 2008. The classification of inherited epidermolysis bullosa (EB): Report of the Third International Consensus Meeting on Diagnosis and Classification of EB. J Am Acad Dermatol 58:931–950.
Fine JD, Eady RA, Bauer EA, Briggaman RA, Bruckner-Tuderman L, Christiano A, Heagerty A, Hintner H, Jonkman MF, McGrath J, McGuire J, Moshell A, Shimizu H, Tadini G, Uitto J. 2000. Revised classification system for inherited epidermolysis bullosa: Report of the Second International Consensus Meeting on diagnosis and classification of epidermolysis bullosa. J Am Acad Dermatol 42:1051–1066.
Foisner R, Feldman B, Sander L, Seifert G, Artlieb U, Wiche G. 1994. A panel of monoclonal antibodies to rat plectin: distinction by epitope mapping and immunoreactivity with different tissues and cell lines. Acta Histochem 96:421–438.
Foisner R, Feldman B, Sander L, Wiche G. 1991. Monoclonal antibody mapping of structural and functional plectin epitopes. J Cell Biol 112:397–405.
Fuchs P, Spazierer D, Wiche G. 2005. Plectin rodless isoform expression and its detection in mouse brain. Cell Mol Neurobiol 25:1141–1150.
Gache Y, Chavanas S, Lacour JP, Wiche G, Owaribe K, Meneguzzi G, Ortonne JP. 1996. Defective expression of plectin/HD1 in epidermolysis bullosa simplex with muscular dystrophy. J Clin Invest 97:2289–2298.
Geerts D, Fontao L, Nievers MG, Schaapveld RQ, Purkis PE, Wheeler GN, Lane EB, Leigh IM, Sonnenberg A. 1999. Binding of integrin alpha6beta4 to plectin prevents plectin association with F-actin but does not interfere with intermediate filament binding. J Cell Biol 147:417–434.
Hieda Y, Nishizawa Y, Uematsu J, Owaribe K. 1992. Identification of a new hemidesmosomal protein, HD1: a major, high molecular mass component of isolated hemidesmosomes. J Cell Biol 116:1497–1506.
Koss-Harnes D, Hoyheim B, Anton-Lamprecht I, Gjesti A, Jorgensen RS, Jahnsen FL, Olaisen B, Wiche G, Gedde-Dahl Jr T. 2002. A site-specific plectin mutation causes dominant epidermolysis bullosa simplex Ogna: two identical de novo mutations. J Invest Dermatol 118:87–93.
Koss-Harnes D, Hoyheim B, Jonkman MF, de Groot WP, de Weerdt CJ, Nikolic B, Wiche G, Gedde-Dahl Jr T. 2004. Life-long course and molecular characterization of the original Dutch family with epidermolysis bullosa simplex with muscular dystrophy due to a homozygous novel plectin point mutation. Acta Derm Venereol 84:124–131.
Koster J, Geerts D, Favre B, Borradori L, Sonnenberg A. 2003. Analysis of the interactions between BP180, BP230, plectin and the integrin alpha6beta4 important for hemidesmosome assembly. J Cell Sci 116(Pt 2):387–399.
Koster J, van Wilpe S, Kuikman I, Litjens SH, Sonnenberg A. 2004. Role of binding of plectin to the integrin beta4 subunit in the assembly of hemidesmosomes. Mol Biol Cell 15:1211–1223.
Krawczak M, Cooper DN. 1991. Gene deletions causing human genetic disease: mechanisms of mutagenesis and the role of the local DNA sequence environment. Hum Genet 86:425–441.
Kunz M, Rouan F, Pulkkinen L, Hamm H, Jeschke R, Bruckner-Tuderman L, Brocker EB, Wiche G, Uitto J, Zillikens D. 2000. Mutation reports: epidermolysis bullosa simplex associated with severe mucous membrane involvement and novel mutations in the plectin gene. J Invest Dermatol 114:376–380.
Laemmli UK. 1970. Cleavage of structural proteins during the assembly of the head of bacteriophage T4. Nature 227:680–685.
Litjens SH, Koster J, Kuikman I, van Wilpe S, de Pereda JM, Sonnenberg A. 2003. Specificity of binding of the plectin actin-binding domain to beta4 integrin. Mol Biol Cell 14:4039–4050.
Litjens SH, Wilhelmsen K, de Pereda JM, Perrakis A, Sonnenberg A. 2005. Modeling and experimental validation of the binary complex of the plectin actin-binding domain and the first pair of fibronectin type III (FNIII) domains of the beta4 integrin. J Biol Chem 280:22270–22277.
McLean WH, Pulkkinen L, Smith FJ, Rugg EL, Lane EB, Bullrich F, Burgeson RE, Amano S, Hudson DL, Owaribe K, McGrath JA, McMillan JR, Eady RA, Leigh IM, Christiano AM, Uitto J. 1996. Loss of plectin causes epidermolysis bullosa with muscular dystrophy: cDNA cloning and genomic organization. Genes Dev 10:1724–1735.
McMillan JR, Akiyama M, Rouan F, Mellerio JE, Lane EB, Leigh IM, Owaribe K, Wiche G, Fujii N, Uitto J, Eady RA, Shimizu H. 2007. Plectin defects in epidermolysis bullosa simplex with muscular dystrophy. Muscle Nerve 35:24–35.
Mellerio JE, Smith FJ, McMillan JR, McLean WH, McGrath JA, Morrison GA, Tierney P, Albert DM, Wiche G, Leigh IM, Geddes JF, Lane EB, Uitto J, Eady RA. 1997. Recessive epidermolysis bullosa simplex associated with plectin mutations: infantile respiratory complications in two unrelated cases. Br J Dermatol 137:898–906.
Nakamura H, Sawamura D, Goto M, Nakamura H, McMillan JR, Park S, Kono S, Hasegawa S, Paku S, Nakamura T, Ogiso Y, Shimizu H. 2005. Epidermolysis bullosa simplex associated with pyloric atresia is a novel clinical subtype caused by mutations in the plectin gene (PLEC1). J Mol Diagn 7:28–35.
Niessen CM, Hulsman EH, Oomen LC, Kuikman I, Sonnenberg A. 1997a. A minimal region on the integrin beta4 subunit that is critical to its localization in hemidesmosomes regulates the distribution of HD1/plectin in COS-7 cells. J Cell Sci 110(Pt 15):1705–1716.
Niessen CM, Hulsman EH, Rots ES, Sanchez-Aparicio P, Sonnenberg A. 1997b. Integrin alpha 6 beta 4 forms a complex with the cytoskeletal protein HD1 and induces its redistribution in transfected COS-7 cells. Mol Biol Cell 8:555–566.
Okumura M, Uematsu J, Hirako Y, Nishizawa Y, Shimizu H, Kido N, Owaribe K. 1999. Identification of the hemidesmosomal 500 kDa protein (HD1) as plectin. J Biochem 126:1144–1150.
Pfendner E, Rouan F, Uitto J. 2005. Progress in epidermolysis bullosa: the phenotypic spectrum of plectin mutations. Exp Dermatol 14:241–249.
Pfendner E, Uitto J. 2005. Plectin gene mutations can cause epidermolysis bullosa with pyloric atresia. J Invest Dermatol 124:111–115.
Pulkkinen L, Rouan F, Bruckner-Tuderman L, Wallerstein R, Garzon M, Brown T, Smith L, Carter W, Uitto J. 1998. Novel ITGB4 mutations in lethal and nonlethal variants of epidermolysis bullosa with pyloric atresia: missense versus nonsense. Am J Hum Genet 63:1376–1387.
Pulkkinen L, Smith FJ, Shimizu H, Murata S, Yaoita H, Hachisuka H, Nishikawa T, McLean WH, Uitto J. 1996. Homozygous deletion mutations in the plectin gene (PLEC1) in patients with epidermolysis bullosa simplex associated with late-onset muscular dystrophy. Hum Mol Genet 5:1539–1546.
Rezniczek GA, de Pereda JM, Reipert S, Wiche G. 1998. Linking integrin alpha6beta4-based cell adhesion to the intermediate filament cytoskeleton: direct interaction between the beta4 subunit and plectin at multiple molecular sites. J Cell Biol 141:209–225.
Rouan F, Pulkkinen L, Meneguzzi G, Laforgia S, Hyde P, Kim DU, Richard G, Uitto J. 2000. Epidermolysis bullosa: novel and de novo premature termination codon and deletion mutations in the plectin gene predict late-onset muscular dystrophy. J Invest Dermatol 114:381–387.
Sawamura D, Goto M, Sakai K, Nakamura H, McMillan JR, Akiyama M, Shirado O, Oyama N, Satoh M, Kaneko F, Takahashi T, Konno H, Shimizu H. 2007. Possible involvement of exon 31 alternative splicing in phenotype and severity of epidermolysis bullosa caused by mutations in PLEC1. J Invest Dermatol 127:1537–1540.
Schaapveld RQ, Borradori L, Geerts D, van Leusden MR, Kuikman I, Nievers MG, Niessen CM, Steenbergen RD, Snijders PJ, Sonnenberg A. 1998. Hemidesmosome formation is initiated by the beta4 integrin subunit, requires complex formation of beta4 and HD1/plectin, and involves a direct interaction between beta4 and the bullous pemphigoid antigen 180. J Cell Biol 142:271–284.
Schneider B, Koppius A, Sedlmeier R. 2007. Use of an exon-trapping vector for the evaluation of splice-site mutations. Mamm Genome 18:670–676.
Schroder R, Furst DO, Klasen C, Reimann J, Herrmann H, van der Ven PF. 2000. Association of plectin with Z-discs is a prerequisite for the formation of the intermyofibrillar desmin cytoskeleton. Lab Invest 80:455–464.
Schröder R, Kunz WS, Rouan F, Pfendner E, Tolksdorf K, Kappes-Horn K, Altenschmidt-Mehring M, Knoblich R, van der Ven PF, Reimann J, Fürst DO, Blümcke I, Vielhaber S, Zillikens D, Eming S, Klockgether T, Uitto J, Wiche G, Rolfs A. 2002. Disorganization of the desmin cytoskeleton and mitochondrial dysfunction in plectin-related epidermolysis bullosa simplex with muscular dystrophy. J Neuropathol Exp Neurol 61:520–530.
Smith FJ, Eady RA, Leigh IM, McMillan JR, Rugg EL, Kelsell DP, Bryant SP, Spurr NK, Geddes JF, Kirtschig G, Milana G, de Bono AG, Owaribe K, Wiche G, Pulkkinen L, Uitto J, McLean WH, Lane EB. 1996. Plectin deficiency results in muscular dystrophy with epidermolysis bullosa. Nat Genet 13:450–457.
Sonnenberg A, Liem RK. 2007. Plakins in development and disease. Exp Cell Res 313:2189–2203.
Steinboeck F, Kristufek D. 2005. Identification of the cytolinker protein plectin in neuronal cells—expression of a rodless isoform in neurons of the rat superior cervical ganglion. Cell Mol Neurobiol 25:1151–1169.
Takahashi Y, Rouan F, Uitto J, Ishida-Yamamoto A, Iizuka H, Owaribe K, Tanigawa M, Ishii N, Yasumoto S, Hashimoto T. 2005. Plectin deficient epidermolysis bullosa simplex with 27-year-history of muscular dystrophy. J Dermatol Sci 37:87–93.
Takizawa Y, Shimizu H, Rouan F, Kawai M, Udono M, Pulkkinen L, Nishikawa T, Uitto J. 1999. Four novel plectin gene mutations in Japanese patients with epidermolysis bullosa with muscular dystrophy disclosed by heteroduplex scanning and protein truncation tests. J Invest Dermatol 112:109–112.
Uitto J, Pfendner E. 2004. Compound heterozygosity of unique in-frame insertion and deletion mutations in the plectin gene in a mild case of epidermolysis bullosa with very late onset muscular dystrophy. J Invest Dermatol 122:A86.
Varki R, Sadowski S, Pfendner E, Uitto J. 2006. Epidermolysis bullosa. I. Molecular genetics of the junctional and hemidesmosomal variants. J Med Genet 43:641–652.
Wiche G. 1998. Role of plectin in cytoskeleton organization and dynamics. J Cell Sci 111(Pt 17):2477–2486.

H. Silm
Clinic of Dermatology, University of Tartu, Estonia

S. Kõks[a,b,c,*]
[a]*Department of Physiology, University of Tartu, Estonia*
[b]*Centre of Translational Medicine, University of Tartu, Estonia*
[c]*Institute of Veterinary Medicine and Animal Sciences, Estonian University of Life Sciences, Estonia*

*Corresponding author at: Department of Physiology, University of Tartu, 19 Ravila Street, 50411 Tartu, Estonia. Tel.: +372 7 374 335; fax: +372 7 374 332
E-mail address: Sulev.Koks@ut.ee (S. Kõks)

27 April 2010

doi:10.1016/j.jdermsci.2010.08.004

Letter to the Editor

ABCA12 dysfunction causes a disorder in glucosylceramide accumulation during keratinocyte differentiation

Harlequin ichthyosis (HI) is an autosomal recessive congenital ichthyoses, and patients of this disease frequently present with severe hyperkeratosis and scales over all of their epidermal surfaces. Recently, the gene encoding ABCA12 was identified as a causative gene for HI [1]. Since dysfunction in ABCA12 causes a decrease in epidermal ceramide (Cer) content concomitantly with loss of the skin lipid barrier, ABCA12 is thought to regulate epidermal generation of Cer. However, so far no direct target of ABCA12 has been identified. Thus, we attempted to study the substrate of ABCA12 by generating an ABCA12-deficient keratinocyte cell line and then comparing its sphingolipid metabolism to that of a normal keratinocyte cell line. Keratinocytes were isolated from a HI patient and a healthy donor [1], then were immortalized by expressing the T-antigen of SV40. After 15 passages, the morphology of the cells became uniform and we confirmed the expression of the SV40 T-antigen by Western blotting (Fig. 1A and B). The cell lines thus generated from the cells isolated from the HI patient and healthy donors were named HIKT and KT1, respectively. Genomic analysis revealed one mutation in the HIKT cells, from A to G adjacent a splice acceptor site of exon 24 (Fig. 1C). This mutation produced two splice variants of 674-bp and 513-pb (Fig. 1D). The 674-bp results from 9-bp lost from exon 24, and the 513-bp results from 170-bp lost from exon 24. This mutation has been reported to seriously affect the function of the ABCA12-protein [1]. We have successfully established an ABCA12-impaired keratinocyte cell line.

Several groups have demonstrated that the expression level of ABCA12 increases during the differentiation of keratinocytes, so that anaplastic keratinocytes express only low levels of ABCA12 [2,3]. As shown in Fig. 2A, anaplastic KT1 scarcely expresses any ABCA12. So, we attempted to induce differentiation of KT1 and HIKT cells, and thereby express high levels of ABCA12 in the cells. We induced differentiation in KT1 and HIKT cells and confirmed the differentiation by measuring the differentiation marker involcurin, which increased significantly in both cell lines during differentiation (3.1-fold increase in KT1 and 2.4-fold increase in HIKT) (Fig. 2A). We further found that ABCA12 also increased during differentiation, with especially high levels of expression at 7 days after induction in the HIKT cells. Following the induction of differentiation in KT1 and HIKT cells, their sphingolipid metabolism was examined at 7 days by labeling the cells with [^{3}H]dihydosphingosine or [^{14}C]galactose (Fig. 2B and C, respectively). Interestingly, apparent accumulations of [^{3}H]GlcCer (Fig. 2B) and [^{14}C]GlcCer (Fig. 2C) were observed in KT1 cells at 7 days post-induction compared to HIKT cells (203% increase at [^{3}H]GlcCer and 181% increase at [^{14}C]GlcCer, respectively). It is noteworthy that [^{14}C]gangliosides levels in KT1 cells were lower rather than equal to levels in HIKT cells (31% reduction), despite the accumulation of GlcCer. Since the ABCA12 is known to localize at lamellar bodies (LBs) in keratinocyte [4], this result indicates that differentiated KT1 cells aggressively accumulate GlcCer in LBs and not in the Golgi apparatus. Our results clearly demonstrate that ABCA12 deficiency impairs the GlcCer accumulation in LBs, thereby strongly indicating that ABCA12 transports GlcCer to the inner leaflet of LBs (Fig. 2D). Mass spectrometer analysis of accumulated

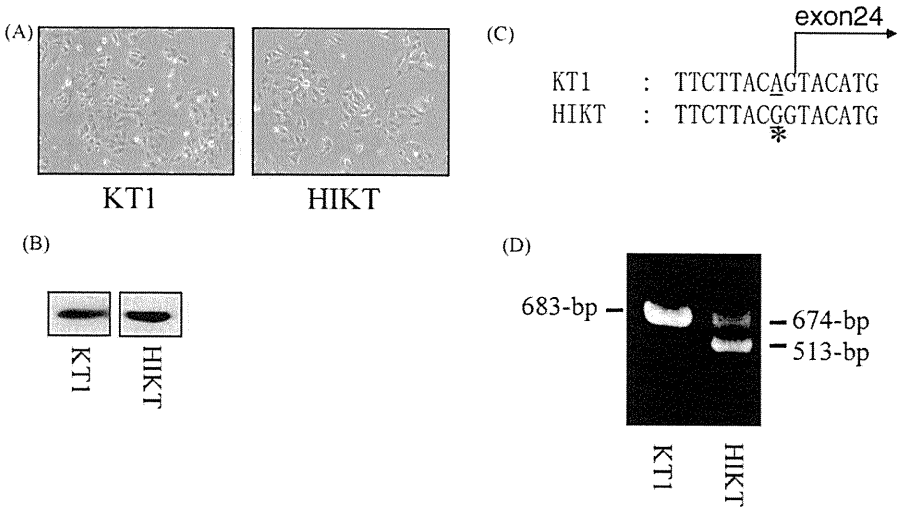

Fig. 1. KT1 and HIKT keratinocyte cell lines. KT1 and HIKT keratinocyte cell lines were generated by introducing the SV40 T-antigen into the cells using the culture supernatant of ΨCRIP-pMFGtsT (distributed from RIKEN cell bank, Tsukuba, Japan). After 15 passages, KT1 and HIKT cells exhibited similar morphology (A), and expected expression levels of T-antigen as examined by Western blotting using anti-SV40 LT (BD biosciences, NJ) (B). Genomic structures of KT1 and HIKT cells neighboring exon 24 (C). *A mutation from A to G in HIKT cells. RT-PCR analysis of mRNA fragments around the exon 23–24 boundary was performed as described previously [1] (D).

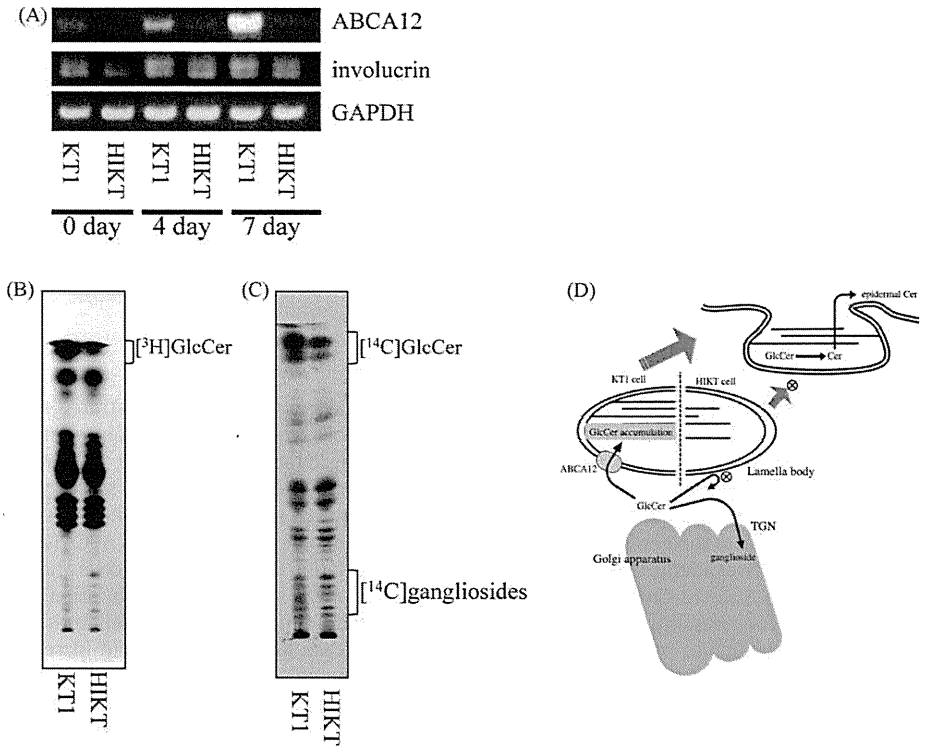

Fig. 2. Sphingolipids in KT1 and HIKT 4 days after induction of differentiation. (A) To induce differentiation, HIKT and KT1 cells were cultured in a DMEM/F-12 (2:1) mixture containing 10% fetal bovine serum, 1.2 mM Ca^{2+}, 10 μg/ml insulin, and 0.4 μg/ml ascorbic acid (differentiation medium) at 39 °C. Before (0 day) and 4 days and 7 days after induction, total RNA was isolated from each cell line, and semi-quantitative RT-PCR was performed using primers for ABCA12, 5′-GAATTGCAAACTGGAAGGAACTCCC-3′ and 5′-GAGTCAGCTAGGATTAGACAGC-3′; for involcurin, 5′-CTCCTCAAGACTGTTCCTCC-3′ and 5′-GCAGTCATGTGCTTTTCCTCTTGC-3′; for GAPDH, 5′-ATCACTGCCACCCAGAAGAC TGTGGA-3′ and 5′-GAGCTTGACAAAGTTGTCATTGAGAGC-3′. Seven days after induction of differentiation, HIKT and KT1 cells (10^6) were metabolically labeled with [^{3}H]dihydrosphingosine (2 μCi) (B) or [^{14}C]galactose (5 μCi) (C), then lipids were extracted and applied to HPTLC plates as described previously [5]. The HPTLC plates were developed with chloroform/methanol/0.05% $CaCl_2$ (60:35:8). The data are representative of tree independent experiments. (D) A possible mechanism of how to generate epidermal ceramides.

GlcCer will provide advanced information about substance preference of ABCA12. This remains for future study.

References

[1] Akiyama M, Sugiyama-Nakagiri Y, Sakai K, McMillan JR, Goto M, Arita K, et al. Mutations in lipid transporter ABCA12 in harlequin ichthyosis and functional recovery by corrective gene transfer. J Clin Invest 2005;115:1777–84.
[2] Jiang YJ, Lu B, Kim P, Paragh G, Schmitz G, Elias PM, et al. PPAR and LXR activators regulate ABCA12 expression in human keratinocytes. J Invest Dermatol 2008;128:104–9.
[3] Jiang YJ, Uchida Y, Lu B, Kim P, Mao C, Akiyama M, et al. Ceramide stimulates ABCA12 expression via peroxisome proliferator-activated receptor {delta} in human keratinocytes. J Biol Chem 2009;284:18942–5.
[4] Yamanaka Y, Akiyama M, Sugiyama-Nakagiri Y, Sakai K, Goto M, McMillan JR, et al. Expression of the keratinocyte lipid transporter ABCA12 in developing and reconstituted human epidermis. Am J Pathol 2007;171:43–52.
[5] Takeda S, Mitsutake S, Tsuji K, Igarashi Y. Apoptosis occurs via the ceramide recycling pathway in human HaCaT keratinocytes. J Biochem 2006;139:255–62.

Susumu Mitsutake[1]
Department of Biomembrane and Biofunctional Chemistry, Faculty of Advanced Life Sciences, Hokkaido University, Nishi 11, Kita 21, Kita-ku, Sapporo 001-0021, Japan

Chihiro Suzuki[1]
Department of Biomembrane and Biofunctional Chemistry, Faculty of Advanced Life Sciences, Hokkaido University, Nishi 11, Kita 21, Kita-ku, Sapporo 001-0021, Japan

Masashi Akiyama
Department of Dermatology, Hokkaido University Graduate School of Medicine, Nishi 7, Kita 15, Kita-ku, Sapporo 060-8638, Japan

Kiyomi Tsuji
Department of Biomembrane and Biofunctional Chemistry, Faculty of Advanced Life Sciences, Hokkaido University, Nishi 11, Kita 21, Kita-ku, Sapporo 001-0021, Japan

Teruki Yanagi, Hiroshi Shimizu
Department of Dermatology, Hokkaido University Graduate School of Medicine, Nishi 7, Kita 15, Kita-ku, Sapporo 060-8638, Japan

Yasuyuki Igarashi*
Department of Biomembrane and Biofunctional Chemistry, Faculty of Advanced Life Sciences, Hokkaido University, Nishi 11, Kita 21, Kita-ku, Sapporo 001-0021, Japan

*Corresponding author at: Hokkaido University, Department of Biomembrane and Biofunctional Chemistry, Graduate School of Pharmaceutical Sciences, Nishi 11, Kita 21, Kita-ku, Sapporo 001-0021, Japan.
Tel.: +81 11 706 9086; fax: +81 11 706 9047
E-mail address: yigarash@pharm.hokudai.ac.jp (Y. Igarashi)

[1]These authors contributed equally to this work.

8 April 2010

doi:10.1016/j.jdermsci.2010.08.012

THE JOURNAL OF IMMUNOLOGY

Human IgG1 Monoclonal Antibody against Human Collagen 17 Noncollagenous 16A Domain Induces Blisters via Complement Activation in Experimental Bullous Pemphigoid Model

Qiang Li, Hideyuki Ujiie, Akihiko Shibaki, Gang Wang, Reine Moriuchi, Hong-jiang Qiao, Hiroshi Morioka, Satoru Shinkuma, Ken Natsuga, Heather A. Long, Wataru Nishie and Hiroshi Shimizu

J Immunol 2010;185;7746-7755; Prepublished online 12 November 2010;
doi:10.4049/jimmunol.1000667
http://www.jimmunol.org/content/185/12/7746

The Journal of Immunology is published twice each month by The American Association of Immunologists, Inc., 9650 Rockville Pike, Bethesda, MD 20814-3994.

Print ISSN: 0022-1767 Online ISSN: 1550-6606.

Human IgG1 Monoclonal Antibody against Human Collagen 17 Noncollagenous 16A Domain Induces Blisters via Complement Activation in Experimental Bullous Pemphigoid Model

Qiang Li,*,[1] Hideyuki Ujiie,*,[1] Akihiko Shibaki,* Gang Wang,* Reine Moriuchi,* Hong-jiang Qiao,* Hiroshi Morioka,† Satoru Shinkuma,* Ken Natsuga,* Heather A. Long,* Wataru Nishie,* and Hiroshi Shimizu*

Bullous pemphigoid (BP) is an autoimmune blistering disease caused by IgG autoantibodies targeting the noncollagenous 16A (NC16A) domain of human collagen 17 (hCOL17), which triggers blister formation via complement activation. Previous in vitro analysis demonstrated that IgG1 autoantibodies showed much stronger pathogenic activity than IgG4 autoantibodies; however, the exact pathogenic role of IgG1 autoantibodies has not been fully demonstrated in vivo. We constructed a recombinant IgG1 mAb against hCOL17 NC16A from BP patients. In COL17-humanized mice, this mAb effectively reproduced a BP phenotype that included subepidermal blisters, deposition of IgG1, C1q and C3, neutrophil infiltration, and mast cell degranulation. Subsequently, alanine substitutions at various C1q binding sites were separately introduced to the Fc region of the IgG1 mAb. Among these mutated mAbs, the one that was mutated at the P331 residue completely failed to activate the complement in vitro and drastically lost pathogenic activity in COL17-humanized mice. These findings indicate that P331 is a key residue required for complement activation and that IgG1-dependent complement activation is essential for blister formation in BP. This study is, to our knowledge, the first direct evidence that IgG1 Abs to hCOL17 NC16A can induce blister formation in vivo, and it raises the possibility that IgG1 mAbs with Fc modification may be used to block pathogenic epitopes in autoimmune diseases. *The Journal of Immunology*, **2010, 185: 7746–7755.**

Bullous pemphigoid (BP) is the most common autoimmune subepidermal blistering disease (1, 2). Circulating autoantibodies target human type XVII collagen (human collagen 17 [hCOL17]), also known as BP Ag 2 (BPAG2) or BP180, which is a major component in hemidesmosome-anchoring filament complexes at the epidermal basement membrane zone (BMZ) (3–9). The major pathogenic epitope of BP autoantibodies is present at the extracellular noncollagenous 16A (NC16A) domain, which has distinctive diversity among different species (10–12). Deposition of anti-hCOL17 autoantibodies at the BMZ triggers sequential inflammatory cascades, including complement activation, degranulation of dermal mast cells, infiltration of eosinophils and neutrophils, and subepidermal blister formation elicited by proteinases derived from the inflammatory cells (13–17).

In the inflammatory mechanism of BP, the IgG-dependent classical complement pathway plays an important role in autoimmune blister formation. Complement components including C1q, C3 and C4 are detected at the dermal-epidermal junction (DEJ) in the skins of patients and experimental BP model mice (17–21). BP phenotypes have been abolished by the inhibition of C1q using neutralizing Abs in experimental models (18). C1q-binding amino acid residues underlie IgG–C1q interaction, which forms an initiation complex in the classical complement pathway (22), such as in humoral immunity to pathogens. The pathogens recognized by Abs are cleared by phagocytosis, Ab-dependent cell-mediated cytotoxicity (ADCC), and complement-dependent cytotoxicity (CDC) mechanisms. Interaction of the C1q and IgG Fc region is an initial step in CDC reaction to pathogens (23). The constant 2 (C_H2) domain is the crucial region for C1q binding to the IgG Fc region (24, 25). Mapping studies of C1q-binding residues have demonstrated that the three spatially close sites (K322, P329, and P331) constitute the binding epicenter in the human IgG1 C_H2 domain. E318 and K320 have been shown to play a minor role in complement activation by site-directed mutagenesis studies in vitro. Among different species, these residues are relatively well conserved (22, 25–27). However, the precise role of these binding residues has not been determined in the activation of complement cascades in vivo.

*Department of Dermatology, Hokkaido University, Graduate School of Medicine, Sapporo; and †Faculty of Medical and Pharmaceutical Sciences, Kumamoto University, Kumamoto, Japan

[1]Q.L. and H.U. contributed equally to this work.

Received for publication February 26, 2010. Accepted for publication October 4, 2010.

This work was supported by the Program for Promotion of Fundamental Studies in Health Sciences of the National Institute of Biomedical Innovation (06-42 to H.S.) and in part by Grants-in-Aid for Scientific Research (A) (21249063 to H.S.) and (C) (20591312 to A.S.) from the Ministry of Education, Culture, Sports, Science, and Technology of Japan.

Address correspondence and reprint requests to Dr. Akihiko Shibaki and Dr. Hiroshi Shimizu, Department of Dermatology, Hokkaido University Graduate School of Medicine, North 15 West 7, Kita-ku, Sapporo, 060-8638, Japan. E-mail addresses: ashibaki@med.hokudai.ac.jp and shimizu@med.hokudai.ac.jp

The online version of this article contains supplemental material.

Abbreviations used in this paper: ADCC, Ab-dependent cell-mediated cytotoxicity; BMZ, basement membrane zone; BP, bullous pemphigoid; C1q, complement 1q; CDC, complement-dependent cytotoxicity; C_H2, constant 2; COL17, type XVII collagen; DB, dilution buffer; DEJ, dermal-epidermal junction; DIF, direct immunofluorescence; Flu, fluorescence; HSC, human serum complement; IIF, indirect immunofluorescence; NC16A, noncollagenous 16A; NHEK, normal human epidermal keratinocyte; PI, propidium iodide; rh, recombinant human; Sf-9, *Spodoptera frugiperda*-9; VH, V region H chain; VL, V region L chain.

www.jimmunol.org/cgi/doi/10.4049/jimmunol.1000667

IgG1 is thought to be the predominant subclass of anti-hCOL17 IgG autoantibodies in sera from BP patients. Clinical studies have shown a preferential detection of hCOL17-specific IgG1 and IgG4 autoantibodies in BP sera, with IgG2 and IgG3 being detected in a minority of patients (5, 7, 28). Eighty-five percent and 46% of BP sera contained IgG1 and IgG4 Abs against hCOL17, respectively (6). The presence of IgG1 autoantibodies has been associated with active BP phenotypes (5, 6), and the autoantibody level has been correlated with the area of skin blistering (29). These clinical findings indicate that IgG1 might be the main pathogenic subclass in BP. However, to our knowledge, there has been no direct in vivo evidence to demonstrate the pathogenic role of the anti-hCOL17 IgG1 autoantibody until now.

To confirm whether BP IgG1 autoantibodies can induce the BP phenotype in vivo and to analyze the importance of various C1q-binding residues in the IgG1 Fc C_H2 domain in BP, we cloned and constructed a recombinant human (rh)IgG1 mAb against hCOL17 NC16A. By site-directed mutagenesis in the C_H2 domain of the IgG1 mAb Fc region, alanine substitutions were introduced at various residue sites that were previously verified as C1q binding sites in vitro. The blister formation triggered by the non-mutated IgG1 mAb was assessed in vivo using our COL17-humanized ($COL17^{m-/-,\ h+}$) mouse model, which expresses hCOL17 but not mouse COL17 at the BMZ (17). In contrast, the IgG1 mAbs that were mutated at the P331 and/or P329 residue(s) failed to elicit blister formation. Our findings indicate that IgG1 Abs, as the predominant IgG subclass, can induce subepidermal blister formation via IgG Fc–C1q interaction in BP.

Materials and Methods

Establishment of the EBV-transformed B cell clones

PBMCs were prepared from seven active nontreated BP patients by density gradient using Ficoll-Paque PLUS (GE Healthcare, Uppsala, Sweden). The diagnosis of BP was made by the typical clinical and histological manifestations as well as by laboratory data including anti-hCOL17 ELISA and indirect immunofluorescence (IIF). The clinical and immunological characteristics of the BP patients are summarized in Supplemental Table I. B cells were isolated by using microbeads conjugated to anti-human CD19 mAb (Miltenyi Biotec, Bergisch Gladbach, Germany), followed by seeding at 15 cells/well in 96 U-bottom microplates (BD Biosciences, San Jose, CA) in complete RPMI 1640 medium containing 2.5 μg/ml ODN2006 (InvivoGen, San Diego, CA) and incubation for 2 wk with irradiated cord mononuclear cells as the feeder layer cells (50,000/well) in the presence of EBV (30% supernatant of B95.8 cells). The culture supernatants were tested for the presence of anti-hCOL17 NC16A Abs by ELISA coated with rhCOL17 NC16A peptide as reported previously (17). The index values of ELISA were defined by the following formula: index = (OD of tested supernatant − OD of negative control)/(OD of positive control − OD of negative control) × 100 (30–32). As a positive control, we used a standard BP serum supplied with the hCOL17 NC16A-ELISA kit (MESACUP BP180 test; Medical and Biological Laboratories, Nagoya, Japan) as reported previously (17, 33). Adjustment of the values relative to the positive control allows comparison of results from different plates, even if performed under different conditions. Positive wells were cloned by limiting dilution in the presence of ODN2006 and irradiated cord mononuclear cells.

Construction of IgG1 expression vector

L chain (κ and λ) and Fd (V region + constant domain 1) fragments were amplified by RT-PCR from monoclonal B cell clones using general primers for the Ab library (Table I), cloned into pCR2.1 vectors (Invitrogen, Carlsbad, CA), and sequenced by ABI 3100 genetic analyzer (Applied Biosystems, Foster, CA). After introducing one cutting site by the restriction endonucleases EcoRV at the 3′ end, the L chain was inserted into the human IgG1 expression vector pAc-κ-Fc or pAc-λ-Fc (Progen, Heidelberg, Germany) at the SacI and EcoRV cutting sites (Supplemental Fig. 1). Then the Fd sequence was inserted into the vector at the XhoI and SpeI cutting sites. The constructed baculovirus vector containing Fd and $V_{\kappa \text{ or } \lambda}$ genes was transfected to *Spodoptera frugiperda*-9 (Sf-9) insect cells using the BaculoGold Transfection Kit (BD Biosciences). Recombinant baculovirus was harvested from the supernatant of Sf-9 cell culture medium TNM-FH (Grace's insect medium, 10% FBS, and penicillin-streptomycin) (Invitrogen) at 4–5 d after the transfection. Secreted rhIgG1 Abs were detected in the supernatant using an hCOL17 NC16A-ELISA kit (MBL, Nagoya, Japan). The whole procedure followed the manufacturers' recommendations.

Production and purification of the rhIgG1 mAb

The recombinant virus inocula, via three rounds of plaque purification, infected Sf-9 cells at a multiplicity of infection of 0.5–10. The cells were grown in SF-900 II SFM (Life Technologies, Carlsbad, CA) serum-free suspension culture using a spinner 1-L flask with a vertical impeller (Corning, Lowell, MA) at 27°C. One week later, supernatant was harvested and clarified by centrifugation and filtered through 0.45 μM filters (Millipore, Bedford, MA). Purification was performed on HiTrap Protein G column (GE Healthcare). The eluted IgG in 1 M glycine-HCl (pH 2.7) was dialyzed in PBS for at least 48 h and then quantified by spectrophotometer (Pharmacia Biotech, Uppsala, Sweden) at 280 nm.

Generation of the mutated IgG1 mAbs

Alanine substitutions were incorporated into the human IgG1 pAc-λ-Fc vector by site-directed mutagenesis using a Quick Change Mutagenesis Kit (Stratagene, La Jolla, CA), according to the manufacturer's instructions. We constructed seven mutants: five single-site ones and two multisite ones. The mutagenic oligonucleotide primers containing target sites are listed in Table I. Primers were purified by PAGE to prevent the primers from experiencing a significant decrease in mutation efficiency. Sequences were verified by ABI 3100 genetic analyzer (Applied Biosystems). The different constructs were expressed in the Sf-9 cells described above. The IgG was directly purified from the filtered serum-free supernatant using 5 ml HiTrap Protein G column (GE Healthcare).

Establishment of hCOL17-293 cells

To establish the hCOL17-293 cell line, FlpIn 293 cells (Invitrogen) were first cotransfected with the constructed plasmid pcDNA5/FRT (Invitrogen) that had been inserted with the hCOL17 gene (a gift from Dr. K. B. Yancey, University of Texas Southwestern Medical Center, Dallas, TX) and pOG44 (Invitrogen) and were then cultured in selective medium (DMEM, 100 μg/ml hygromycin B [Invitrogen], and 10% FBS). Second, the expression levels of hCOL17 were detected by Western blot analysis using BP serum Abs (1:20) as the first Ab. Eventually, the positive clones were maintained in DMEM containing 50 μg/ml hygromycin B and 10% FBS. The procedures were handled according the manufacturers' recommendations.

Epitope mapping of the IgG1 mAb

We synthesized the N terminus half (hNC16A 1–3, aa 490–534) of the hCOL17 NC16A domain as a GST-fusion protein using the expression vector pGEX2-T (Amersham Biosciences, Uppsala, Sweden) and bacteria B12 (Amersham Biosciences), as reported previously (17, 34). Other peptides including hNC16A 1 (aa 490–506), hNC16A 2 (aa 506–520), hNC16A 2.5 (aa 514–532), and hNC16A 3 (aa 520–534) were expressed in the same way and then purified with a GSTrap FF affinity column (GE Healthcare). The purified IgG1 mAb 3.B6 (0.25 μg/ml) was incubated with the 0.5 μg/lane GST-fusion proteins that were transferred to a 0.2-μm nitrocellulose membrane (Bio-Rad, Richmond, CA) for storage at 4°C overnight. Immunoblots were probed with anti-human IgG polyclonal Abs conjugated with HRP (1:1000; DakoCytomation, Glostrup, Denmark). BP serum from patient 3 (1:30) was acted as the positive control.

Competitive-inhibition assay

Competitive-inhibition ELISA was performed in triplicate as described previously (35). Inhibitor solutions (five subpeptides of the hNC16A, full-length hNC16A, and GST protein) were double serially diluted in 0.5% BSA and mixed with equal volumes of the IgG1 mAb 3.B6 (2.5 μg/ml), then incubated at 37°C for 1 h. One hundred microliters of the mixtures was added to the wells coated with hCOL17 NC16A. The remainder of the assay was performed according to standard procedures. OD was measured at 450 nm.

C1q-binding assay

The C1q-binding activity of the mutated IgG1 mAbs was determined by C1q ELISA-binding assay. The mAbs with double serial dilution (starting concentration: 20 μg/ml) in 0.05 M sodium carbonate buffer (pH 9) were coated in a 96-well plate (Nalge Nunc International, Rochester, NY) and left overnight at 4°C. The plates were washed three times with PBS containing 0.05% Tween 20 and blocked for 1 h at room temperature with

ELISA diluent buffer (BD Biosciences), then incubated for 2 h with 100 μl 4 μg/ml human complement component C1q (Sigma-Aldrich, St. Louis, MO) in ELISA diluent buffer. Then, 100 μl of a 1:400 dilution of sheep polyclonal to C1q (HRP) (Abcam, Tokyo, Japan) was added after washing, and incubation was done for 1 h. Plates were washed five times and displayed in tetramethylbenzidine-soluble reagent (ScyTek, Logan, UT) and then stopped by the addition of 50 μl 20% H_2SO_4 (Wako, Osaka, Japan). The OD was determined at 450 nm. To correct for background, the OD at 450 nm was subtracted from the OD at 620 nm. Binding activity was calculated by the following formula: index value = $(OD_{test} - OD_{blank})/(OD_{St.} - OD_{blank})$, where St. is standard human IgG1 (BD Biosciences) and blank is the diluent buffer.

CDC assay

Serum complements from human (Quidel, San Diego, CA) and mouse (Innovative, Novi, MI) were used for cytotoxicity assay. The mAbs (20–0.04 μg/ml) were diluted with dilution buffer (DB) (DMEM [Life Technologies] [pH 7.2], 2 mM glutamine, 0.1% BSA, and 50 μg/ml hygromycin). The hCOL17-293 cells were washed in DB and resuspended at a density of 10^6 cells/ml. In a typical assay, 50 μl of the mAbs, 50 μl diluted complement, and 50 μl cell suspension were added to flat-bottom tissue culture 96-well plates. The mixture was incubated for 2 h at 37°C in 5% CO_2 incubator to facilitate cell lysis. Then, 50 μl Alamar Blue (Invitrogen) diluted in the DB was added to each well and incubated overnight at 37°C in 5% CO_2 incubator. Fluorescence (Flu) value was monitored at 530-nm excitation wavelength and 630-nm emission wavelength using a 96-well Fluorometer (Berthold, Tokyo, Japan). Reduced Flu units exhibit proportionally to the number of viable cells. The activity of the various mutants was examined by plotting the percent CDC activity against the log of working concentration of the mAb. The Flu value of triplicates was used to calculate the percent cytotoxicity: percent CDC activity = $100 \times (1 - [Flu_{no\ complement} - Flu_{test}]/[Flu_{no\ complement} - Flu_{total\ lysis}])$, where $Flu_{total\ lysis}$ reading from positive control well was incubated for an additional 15 min with lysis solution (Roche, Mannheim, Germany).

ADCC assay

The normal PBMCs were fractionated by Ficoll-Paque PLUS gradient and resuspended in assay reaction buffer (RPMI 1640, 10 mM HEPES, 1% FBS, and 100 μg/ml gentamycin). The hCOL17-293 cells were washed and resuspended in the assay reaction buffer. Double-serial-diluted mAb in a 50-μl assay reaction buffer was incubated with 50 μl target cells (hCOL17-293 cells) (10,000 cells/well) for 30 min at 37°C. Then 50 μl effector cells (normal PBMCs) in a cell suspension (100,000 cells/well) was dispensed into the wells, and incubation was continued for 4 h at 37°C. The activity of lactate dehydrogenase was determined by using the Cytotoxicity Detection PLUS (lactate dehydrogenase) Kit (Roche), according to the manufacturer's instructions. The absorbance (450 nm) of triplicates was used to calculate the percent cytotoxicity: percent cytotoxicity = $100 - 100 \times (OD_{test} - OD_{background})/(OD_{total\ lysis} - OD_{background})$, where $OD_{total\ lysis}$ reading from the positive-control well was incubated for an additional 15 min by lysis solution (Roche).

Passive-transfer models

The Abs including the nonmutated, mutated, BP and healthy serum IgGs were individually injected into 1-d neonatal COL17-humanized ($COL17^{m-/-,\ h+}$) mice at a dose of 25–200 μg/g body weight as described previously (17). At 48 h after i.p. injection of the IgG Abs, skin blister formation was assessed by gentle skin friction. Back skin was used for histological examination (Genetic-Lab, Sapporo, Japan) and direct immunofluorescence (DIF) test using FITC-conjugated polyclonal Ab to human IgG (1:100) (DakoCytomation), murine C1q (1:40) (MBL), and murine C3 (1:200) (Abcam).

Immunofluorescence

Immunofluorescence analysis using the nonmutated or mutated IgG1 mAbs was performed on adult $COL17^{m-/-,\ h+}$ mouse tail, neonatal $COL17^{m-/-,\ h+}$ mouse skin, and normal human skin as described previously (17). Flu labeling was performed with FITC-conjugated secondary Abs (1:100) (DakoCytomation), followed by 10 μg/ml propidium iodide (PI) (Sigma-Aldrich) to counterstain the nuclei. The stained samples were observed and photographed under a confocal laser scanning microscope (Olympus Fluoview FV1000; Olympus, Tokyo, Japan).

Ethical considerations

This study was approved by the Institutional Review Board of Hokkaido University (Sapporo, Japan) and fully informed consent from all patients was obtained for use of human material. All animal operations were approved by and performed in accordance with the Institutional Lab Animal Care and Use Committee of Hokkaido University.

Statistics

Data values were shown as means and/or percentages. We determined statistical significance using Student t test or Pearson χ^2 test. One-way or two-way ANOVA test was used for comparing the C1q-binding, CDC, and ADCC activities of the nonmutated and mutated mAbs. A p value <0.05 or 0.01 was considered statistically significant. Analysis was carried out using the statistical software SPSS 10.0 (SPSS, Chicago, IL).

Results

Establishment of immortalized B cell clones derived from BP patients

By means of EBV transformation and limiting dilution (36), three immortalized B cell clones (3.B6, 1.F5, and 7.H8) were established from PBMCs of the seven active BP patients (3.B6 from patient 3, 1.F5 from patient 1, and 7.H8 from patient 7). These three clones stably grew and secreted the IgG mAbs against hCOL17 NC16A. ELISA analysis showed that all the supernatants from the three clones (3.B6, 1.F5, and 7.H8) recognized the rhCOL17 NC16A protein (respective index values [mean ± SD]: 82.99 ± 4.32, 40.18 ± 2.53, and 30.79 ± 1.61). The IgG subclasses of the three clones are IgG1, IgG1, and IgG4, respectively, as determined by gene sequencing. IIF analysis using normal human skin revealed that the supernatants of both 3.B6 and 1.F5 showed linear IgG deposition at the BMZ (Fig. 1*A*, 1*B*). In contrast, the supernatant of clone 7.H8 failed to recognize the BMZ (Fig. 1*C*). We then generated rhIgG1 mAbs containing the Fab regions of these three immortalized B cell clones.

Generation of rhIgG1 mAbs against hCOL17 NC16A

To construct rhIgG1 mAbs, we amplified and cloned the cDNA that encodes IgG L and H chain variable domains ($V_{\kappa\ or\ \lambda}$ and Fd) from the immortalized B cell clones by RT-PCR using Ab library general primers (Table I). The 700-bp L/H chain variable genes (VL/VH) of clones 3.B6, 1.F5, and 7.H8 were cloned and ampli-

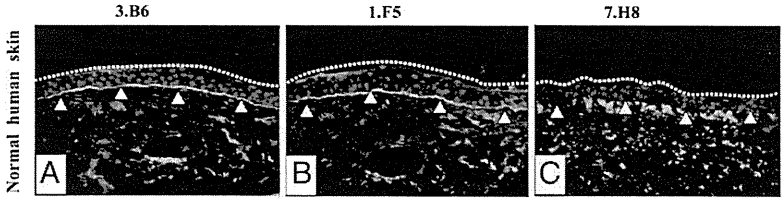

FIGURE 1. Characterization of immortalized B cell clones. IIF analysis was used for detecting the immunoreactivity of the IgG supernatant collected in the first week with normal human skin. Rabbit polyclonal Abs against the H and L chains of human IgG (DakoCytomation) conjugated with FITC were used as secondary Abs (1:100). IgG in the diluted supernatant (1:1) from 2 clones 3.B6 (*A*) and 1.F5 (*B*) deposits linearly (green, FITC) at the DEJ (white arrowheads) (skin surface, white dotted line). Negative staining is observed from clone 7.H8 (*C*). Cell nuclei (red) were counterstained with PI. Original magnification ×200 (*A–C*).

Table I. *General RT-PCR primers for cloning variable genes (V) and the mutagenic primers for substituting alanines at C1q binding sites*

Primers for κ-chain	
HK5	GAMATYGAGCTCACSCAGTCTCCA
HK3	GCGCCGTCTAGAACTAACACTCTCCCCTGTTGAAGCTCTTTGTGACGGGCAAG
Primers for λ-chain	
HL5	CASTYTGAGCTCACKCARCCGCCCTC
HL3	GAGGGATCTAGAATTATGAACATTCTGTAGG
Primers for Fd	
$H_{1,3}$	CAGGTGCAGCTGGTGSAGTCTGG
H_2	CAGGTCAACTTGAAGGAGTCTGG
H_4	CAGGTGCAGCTGCAGGAGTCGGG
V_H5	CAGGTGCAGCTCGAGSAGTCTGG
HG3	GCATGTACTAGTTTTGTCACAAGA
Single-site mutagenic primers	
E318→A	TGGCTGAATGGCAAGGCGTACAAGTGCAAGGTC
K320→A	GCTGAATGGCAAGGAGTACGCGTGCAAGGTCTCCAACAAA
K322→A	GCAAGGAGTACAAGTGCGCGGTCTCCAACAAAGCCC
P329→A	CAACAAAGCCCTCGCAGCCCCCATCGA
P331→A	AGCCCTCCCAGCCGCCATCGAGAAAACC
Multisite mutagenic primers	
E318A K320A K322A	GACTGGCTGAATGGCAAGGCGTACGCGTGCGCGGTCTCCAACAAAGCCCTC
P329A P331A	CAACAAAGCCCTCGCAGCCGCCATCGAGAAAAC

General primers for V_L and Fd chains (M = A, C; Y = C, T; S = G, C; K = G, T; R = A, G). Mutagenic primers at C1q binding sites (only showing the sense primer; the underlined codons are substituted into alanines).

fied by the V_λ/$VH_{1,3}$ V_κ/VH_2, and V_κ/$VH_{1,3}$ subfamily primers, respectively (Table II). Details of the variable gene sequence from the clones are summarized in Supplemental Table II.

Both the VL and VH genes were successively cloned into XhoI/SpeI and SacI/EcoRV sites of the pAc-κ-Fc or pAc-λ-Fc baculovirus IgG1 expression vectors (Supplemental Fig. 1) (37). Recombinant baculovirus was produced by transfecting the recombinant vectors that contained VL/VH genes into Sf-9 insect cells. Postinfection with the purified recombinant baculovirus, the Sf-9 cells secreted rhIgG1 mAbs in the culture supernatant. ELISA analysis showed that the rIgG1 mAb from the clone 3.B6 recognized hCOL17 NC16A (index value [mean ± SD]: 161 ± 5.37) but not the unrelated control protein, human type VII collagen (index value: 2.2 ± 0.04). The human COL17 NC16A ELISA index values of mAbs derived from clones 1.F5 and 7.H8 were 4.23 ± 0.02 and 1.74 ± 0.01, respectively, which are significantly lower than that of clone 3.B6 ($p < 0.01$). This result indicates that the reactivity and/or affinity of IgG Abs secreted from insect cells was altered from those produced by human B cells, possibly as a result of differences in three-dimensional structure, to glycosylation or to other factors, even if the Abs had the same gene sequences as the variable regions (38, 39). For example, N-deglycosylation was even observed to affect the m.w. of the H or L chains of Ch-K20-sf9 (37). IIF analysis demonstrated that the rIgG1 mAb 3.B6 reacted with the BMZ of normal human (Fig. 2*A*) and COL17-humanized ($COL17^{m-/-,\ h+}$) mouse skin (Fig. 2*B*) but not with the wild-type mouse skin (Fig. 2*C*).

The amount of the mAb 3.B6 in the supernatant of the infected Sf-9 cells ranged from 5 to16 μg/ml, values that were determined by sandwich ELISA using sheep anti-human Fab Abs. Kinetic analysis using the Biacore system demonstrated that the mAb 3.B6 had high affinity for $K_D = 5.3 \times 10^{-9}$ M ($K_d = 1.9 \times 10^{-4}$ 1/s; $K_a = 3.6 \times 10^4$ 1/Ms; $K_D = K_d/K_a$). The purified mAb 3.B6 stained the cell surface of the normal human epidermal keratinocytes (Fig. 2*D*) and 293 cells that had been transfected with the hCOL17 gene (Fig. 2*E*), suggesting that this mAb recognizes the extracellular domain of hCOL17.

Table II. *Usage of Ab general primers for cloning variable genes from the B-cell clones*

B Cell Clone	L Chain	VL Subfamily	H Chain	VH Subfamily
3.B6	V_λ	VL1-JL3b	$VH_{1,3}$	VH1-D4-JH6
1.F5	V_κ	VK1-JK3	VH_2	VH2-D6-JH4
7.H8	V_κ	VK1-JK2	$VH_{1,3}$	VH3-D5-JH6

Epitope mapping by Western blot analysis using the rNC16A subpeptides revealed that the mAb 3.B6 specifically reacted with the full-length hNC16A, hNC16A 1–3, hNC16A 2, and hNC16A 2.5 (Fig. 3*A*, 3*B*). Binding inhibition assays demonstrated that two peptides (hNC16A 2 and hNC16A 2.5) sharing seven amino acids inhibited the binding of mAb 3.B6 to the hNC16A in a dose-dependent manner (Fig. 3*C*). Thus, the mAb 3.B6 specifically recognized an epitope present at subregion 2 of the hNC16A domain, which was also recognized by the serum derived from the same donor (patient 3) (Fig. 3*B*).

Generation of rhIgG1 mAbs with mutations at C1q binding sites and characterization of C1q-binding activity

After the binding activity of the IgG1 mAb 3.B6 was verified, site-directed mutagenesis was introduced at the C1q binding sites in the C_H2 domain of the rhIgG1 Fc region. Five independent residues (E318, K320, K322, P329, and P331) were substituted with alanine by single-site or multisite (E318 K320 K322 or P329 P331) mutation in the C_H2 domain. Both IIF and Western blot analysis demonstrated that all the mutated mAbs reacted to the hCOL17 NC16A as specifically as the nonmutated mAb did (data not shown). Kinetic analysis also demonstrated that the mutated mAbs had similar affinity with the nonmutated IgG1 mAb 3.B6 (data not shown).

In contrast, all the mutated mAbs demonstrated significantly reduced binding ability to C1q compared with that of the nonmutated mAb ($p < 0.01$) (Fig. 4). The binding abilities of E318A and K320A were slightly lower than that of the nonmutated mAb. No significant difference was observed between the two mutated mAbs ($p > 0.05$). The K322A, E318A K320A K322A, and P329A mAbs showed half the binding ability of the nonmutated mAb. There were no significant differences among these three mAbs ($p > 0.05$). Alanine substitution at position P331 or P329 P331 seemed to demonstrate the lowest C1q-binding capacity of

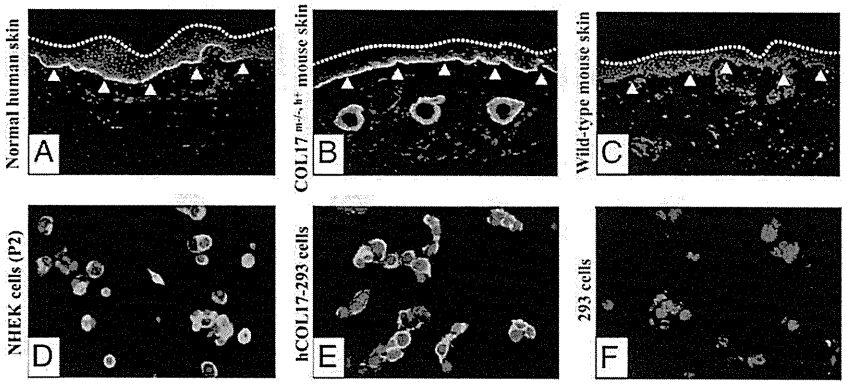

FIGURE 2. Characterization of rhIgG1 mAb 3.B6. Analysis on the specificity of mAb by IIF assay shows that the mAb (green, FITC) deposits linearly at the DEJ (white arrowheads) (skin surface, white dotted line) of normal human (*A*) and COL17-humanized ($COL17^{m-/-,h+}$) mouse skin (*B*), but does not deposit in the wild-type mouse skin (*C*). At the cellular level, the mAb binds to the plasma membrane (green) of second-passage normal human epidermal keratinocytes (NHEKs, P2) (*D*) and hCOL17-293 cells (*E*), but does not bind to 293 cells (negative control) (*F*). Red shows nuclear staining by PI. Original magnification ×100 (*A–C*); ×400 (*E, F*).

any of the mutated mAbs. These data indicate that P331 is the most important residue for IgG1 Fc–C1q interaction, followed by the P329, K322, K320, and E318 binding sites in the C1q-binding motif of the Fc C_H2 domain.

In vitro characterization of the CDC and ADCC activities of the mutated IgG1 mAbs

To test the ability of the mutated IgG1 mAbs to activate complement cascade in vitro, CDC assay was carried out using the hCOL17-293 cells as target cells. At 1:20 dilution of human serum complement (HSC), the nonmutated mAb showed the highest CDC activity (Fig. 5*A*). The CDC activity of the two mutated mAbs (E318A and K320A) was nearly half that of the nonmutated mAb, followed in decreasing order by K322A, E318A K320A K322A, and P329A. Their CDC activity was about one-third that of the nonmutated mAb. The mutants P331A and P329A P331A showed very low CDC activity. When the HSC concentration was increased, the percentage of CDC activity increased in the mutants E318A, K320A, K322A, P329A, and E318A K320A K322A (Fig. 5*B*, 5*C*). In contrast, no obvious change was observed in the CDC activity for P331A or P329A P331A, even at the highest HSC concentration (Fig. 5*C*). Similar results were shown when mouse serum complement was used instead of HSC (Fig. 5*D–F*). Taken together, these results indicate that all five residues of the IgG1 C_H2 domain play at least moderate roles and that P331 is the most important residue for activating complements in vitro.

To further investigate whether these mutations affect the Fc-FcγR–mediated ADCC activity of the IgG1 mAbs, we analyzed the mutated mAbs for ADCC activity using the hCOL17-293 cells as target cells and normal PBMCs as effector cells. The mutated mAbs (E318A, K320A, K322A, and E318A K320A K322A) exhibited ADCC activity similar to that of the nonmutated mAb

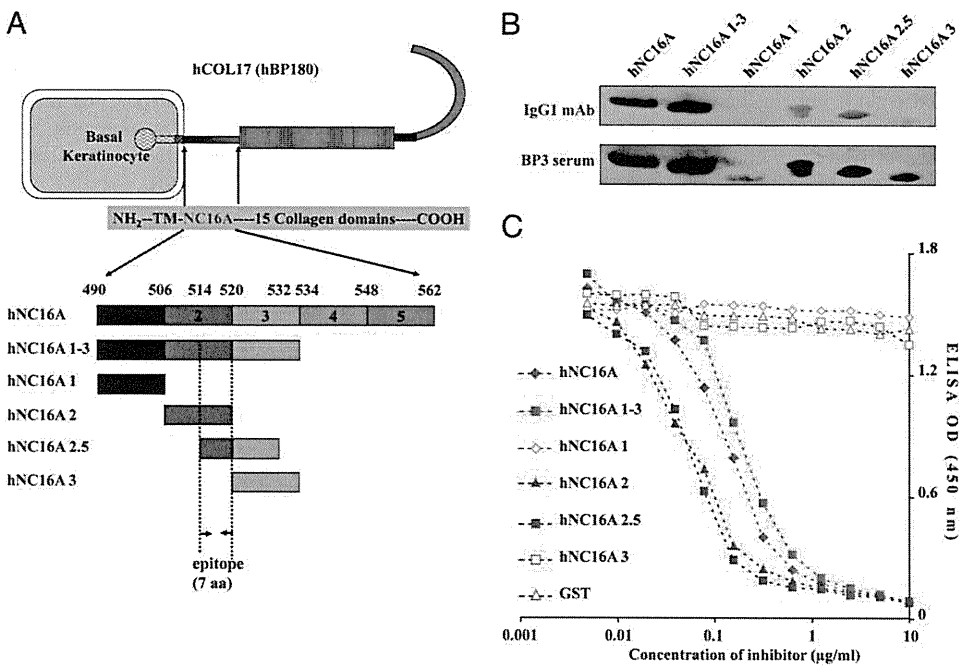

FIGURE 3. Epitope mapping of the IgG1 mAb 3.B6. A schematic map of hCOL17 (hBP180) showing the location of the hNC16A domain and the subpeptides synthesized for epitope mapping studies (*A*). Western blot analysis reveals that the IgG1 mAb recognizes the following subpeptides: hNC16A full-length (aa 490–562), hNC16A 1–3 (aa 490–534), hNC16A 2 (aa 506–520), and hNC16A 2.5 (aa 514–532) (*B*). Two subpeptides (hNC16A 1 and 3) other than the abovementioned four are also recognized by the BP serum from the same donor (patient 3). In ELISA inhibition assay (*C*), the IgG1 mAb 3.B6 (2.5 μg/ml) was incubated with the five subpeptides as inhibitor (10–0.005 μg/ml), with GST protein acting as negative control and hNC16A acting as positive control. The index value of the binding of mAb 3.B6 to the full-length hNC16A was detected by ELISA at OD 450 nm. The three subpeptides (hNC16A 1–3, hNC16A 2, and hNC16A 2.5) almost completely inhibited the binding activity of the IgG1 mAb 3.B6 in a dose-dependent manner. No significant difference in mean inhibitory activity was observed among the three subpeptides ($p > 0.05$ by two-way ANOVA test).

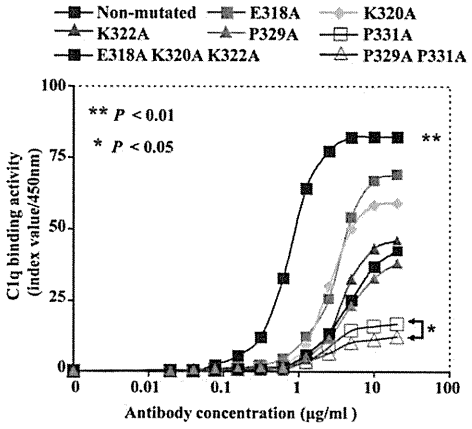

FIGURE 4. C1q-binding activity of the mutated IgG1 mAbs. The ELISA Index value of C1q binding increases gradually with increases in the IgG1 Ab. Maximal binding activity in descending order is nonmutated, then E318A, K320A, K322A, E318A K320A K322A, P329A, P331A and P329A P331A mutated mAbs. Mean index value is higher for the non-mutated mAb than for any other mutated mAbs ($p < 0.01$ by two-way ANOVA test). There is no significant difference in mean index value for E318A versus K320A or for K322 versus E318A K320A K322A or P329A ($p > 0.05$ by one-way ANOVA test). Significant difference is seen between P331A and P329A P331A ($p < 0.05$ by one-way ANOVA test).

(Fig. 6). In contrast, the substitutions at P329 or P329 P331 almost completely eliminated the ADCC activity of the mAbs ($p < 0.01$). Alanine substitution at the P331 site partially decreased the ADCC activity ($p < 0.05$). Altogether, these results suggest that P329 is a critical residue for IgG1–FcγR interaction in vitro.

In vivo functional characterization of the nonmutated and mutated IgG1 mAbs using a COL17-humanized (COL17$^{m-/-,\ h+}$) BP mouse model

To investigate the pathogenic activity of the nonmutated and mutated IgG1 mAbs in vivo, we performed a passive-transfer experiment using neonatal COL17-humanized (*COL17$^{m-/-,\ h+}$*) mice that we had established recently (17). Forty-eight hours after i.p. injection of the nonmutated IgG1 mAb (200 μg/g body weight), eight of nine neonatal mice became erythematous and showed BP-like skin blistering by gentle skin friction (Fig. 7*A*, Table III). Histopathologic examination of the recipient mouse skin confirmed the formation of subepidermal blistering (Fig. 7*B*), infiltration of lymphocytes and neutrophils (Fig. 7*C*), and degranulation of mast cells (Fig. 7*D*). DIF examination revealed the linear deposition of human IgG (Fig. 8*A*) at the BMZ, as well as of mouse C1q (Fig. 8*B*) and C3 (Fig. 8*C*). Administration of the lower dose of the nonmutated IgG1 mAb (100, 50, or 25 μg/g body weight) resulted in a lower frequency of phenotypic changes (five of seven, four of seven, or zero of five mice, respectively) (Table III). ELISA analysis of the sera of recipient mice revealed that the mean index value of the circulating anti-hCOL17 NC16A IgG1 mAbs declined from 55.39 (200 μg/g body weight) to 43.74, 36.91, and 26.53 (100, 50, and 25 μg/g body weight, respectively). Similar results were observed in positive control models with BP patients' IgG autoantibodies (data not shown) in which the BP phenotype was induced as described previously (17).

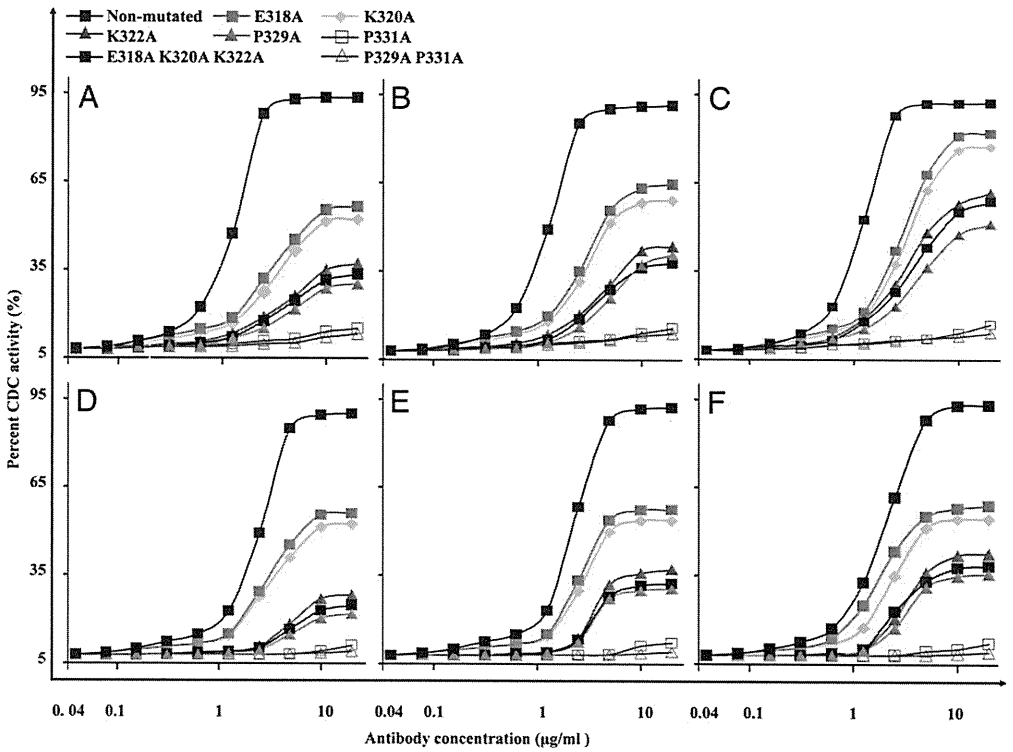

FIGURE 5. Characterization of in vitro CDC activity for the mutated IgG1 mAbs. The nonmutated mAb has the highest percent CDC activity ($p < 0.01$ by one-way ANOVA test) at HSC dilution of 1:20 (*A*), 1:10 (*B*), and 1:5 (*C*), as well as at murine serum complement dilutions of 1:20 (*D*), 1:10 (*E*), and 1:5 (*F*). E318A and K320A have significantly higher CDC activity than K322A, P329A, and E318A K320A K322A ($p < 0.01$ by two-way ANOVA test). No significant difference in the mean percent activity is seen for E318A versus K320A or for K322A versus P329A or versus E318A K320A K322A ($p > 0.05$ by one-way ANOVA test). P331A and P329A P331A show no CDC activity. Significant differences are seen for the two mAbs versus the other mAbs ($p < 0.01$ by two-way ANOVA test).

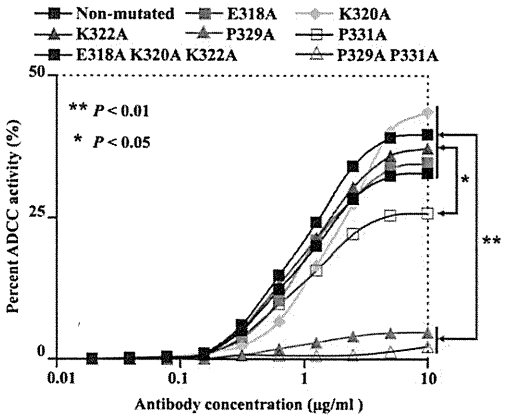

FIGURE 6. Characterization of in vitro ADCC activity for the mutated IgG1 mAbs. In IgG1 mAb-dependent cell-mediated cytotoxicity (ADCC) assay, normal human PBMCs were applied as the effector cells, and hCOL17-293 cells were the target cells. No significant differences in ADCC percent activity are shown for the E318A, K320A, K322A, and E318A K320A K322A versus the nonmutated mAbs ($p > 0.01$ by one-way ANOVA test). ADCC activity is higher for these four mAbs than for P331A ($p < 0.05$ by two-way ANOVA test). The mAbs P329A and P329A P331A show almost no ADCC activity, and significance differences are observed versus the others and nonmutated mAb ($p < 0.01$ by two-way ANOVA test).

In contrast, IgG1 mAbs with the double-site mutation (P329A P331A) completely failed to induce the BP phenotype (zero of eight mice) at the highest dose (200 μg/g body weight), whereas IgG1 mAbs with single-site mutation (P329A or P331A) showed significantly reduced pathogenic capability (one of seven or one of eight mice, respectively) compared with nonmutated IgG1 mAb ($p < 0.01$) (Figs. 7*I–L*, 8*G–I*, Table III). The other three IgG1 mAbs with a single-site mutation (E318A, K320A, or K322A) that showed high or moderate complement activity in vitro elicited skin detachment in the majority of mice at the highest dose (200 μg/g body weight) and demonstrated pathogenic activities in a dose-dependent manner as was true for the non-mutated IgG1 mAb (Figs. 7*E–H*, 8*D–F*). There were no significant differences in positive ratio of skin detachment between these three mAbs and the nonmutated mAb ($p > 0.05$) (Table III). No significant differences were observed in the hCOL17 NC16A-ELISA index values (mean values) of the circulating human IgG Abs in the recipient sera among the mutated or nonmutated IgG1 mAb models at the dose of 200 μg/g body weight ($p > 0.01$).

Discussion

This study provides, to our knowledge, the first direct evidence that human IgG1 Abs against hCOL17 NC16A can induce subepidermal blisters in vivo. BP phenotypic features, including dermal-epidermal separation, deposition of IgG1 Abs C1q and C3, recruitment of neutrophils, and degranulation of mast cells, were successfully reproduced in COL17-humanized ($COL17^{m-/-,\ h+}$) mice by the administration of human IgG1 mAbs against human COL17 NC16A, although the components of the immune system, such as complements and inflammatory cells, are still of murine origin in this experimental model.

It is well known that various IgG subclasses have distinct functional properties. IgG1 and IgG3 are the most effective complement activators, whereas IgG4 is not capable of fixing complements (40). Previous clinical studies demonstrated that IgG1 and IgG4 autoantibodies are major IgG subclasses of BP patient autoantibodies and that IgG2 and IgG3 are minor subclasses of BP patient autoantibodies (5, 7, 28). In vitro analysis using cryosections of human skin and leukocytes from healthy volunteers demonstrated that IgG1 autoantibodies purified from BP sera showed much stronger pathogenic activity than that of IgG4 autoantibodies (41). However, there has been no direct evidence of pathogenic activity of IgG1 autoantibodies in a BP model in vivo. Our group and others have successively reproduced BP phenotypes in COL17-humanized mice by administering IgG autoantibodies prepared from BP patients (15, 17). However, these autoantibodies were poly-

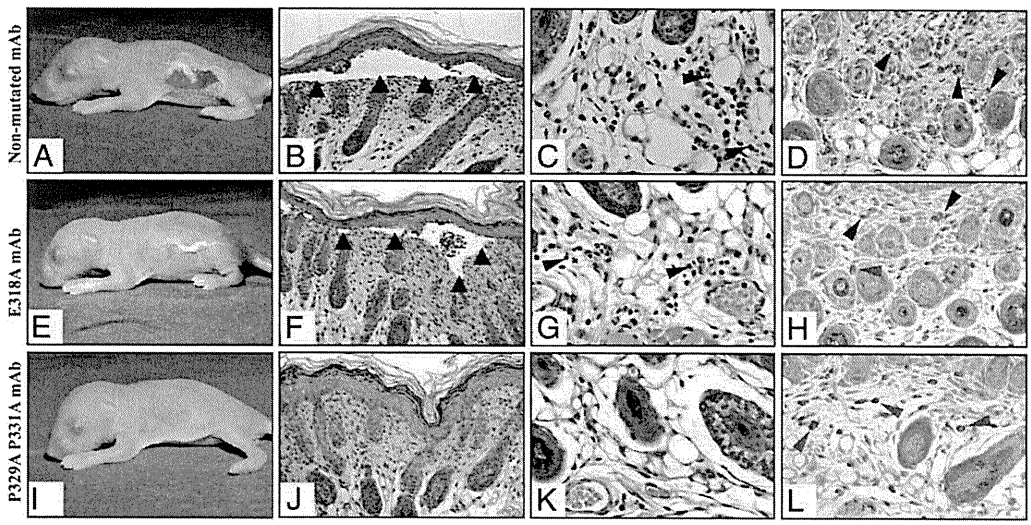

FIGURE 7. Pathogenic activity in vivo of the nonmutated and mutated IgG1 mAbs. The neonatal COL17-humanized ($COL17^{m-/-,\ h+}$) mice were i.p. injected with the nonmutated IgG1 mAb (200 μg/g body weight) or the mutated IgG1 mAbs E318A and P329A P331A (200 μg/g body weight). Forty-eight h later, pathogenic activity was determined by skin blistering test and histology biopsy of back skin including H&E and toluidine blue staining. Skin blistering is positive for the nonmutated and E318A mAbs models (*A*, *E*) and negative for the P329A P331A model (*I*). H&E staining shows epidermal detachment (black arrowheads) at the DEJ in the nonmutated (*B*) and E318A (*F*) mAbs models but not in the P329A P331A model (*J*). The numbers of neutrophils (black arrowheads) and degranulated mast cells (black arrowheads) infiltrating the dermis are more greatly reduced in the P329A P331A (*K*, *L*) model than in the nonmutated (*C*, *D*) and E318A (*G*, *H*) models. Red arrowheads indicate normal undegranulated mast cells. Original magnification ×100 (*B*, *F*, *J*); ×200 (*D*, *H*, *L*); ×400 (*C*, *G*, *K*).

Table III. *Pathogenic activity of the non-mutated and mutated IgG1 mAbs against hCO17 NC16A in the COL17-humanized* (COL17$^{m-/-,h+}$) *BP mouse model*

Abs	Mice with Skin Detachment[a], for Each Injection Dosage (μg/g Body Weight)			
	200 μg	100 μg	50 μg	25 μg
Nonmutated	8/9	5/7	4/7	0/5
Mutated				
E318A	4/6	2/5	0/5	0/4
K322A	5/8	2/6	1/6	1/5
E318A K320A K322A	3/7	2/6	0/5	0/5
P329A	1/7	1/5	0/4	0/5
P331A	1/8	0/7	0/6	0/5
P329A P331A	0/8	0/5	0/4	0/6
Normal human[b]	0/6	—	—	—

[a]Skin blistering test performed at 48 h in neonatal mice.
[b]Human IgG purified from serum in single normal volunteer.

clonal IgG containing all four IgG subclasses. In this study, we have directly demonstrated that anti-hCOL17 NC16A IgG1 mAb has pathogenic activity in vivo by using COL17-humanized (*COL17*$^{m-/-,\ h+}$) BP model mice. As previous clinical studies on BP (5, 7, 28), our results further support the notion that IgG1 autoantibodies against hCO17 are potent and possibly the main pathogenic IgG autoantibodies in BP.

Previous studies have demonstrated that activation of the complement pathway is a pivotal step in the BP pathomechanism (17, 18, 42). By comparing nonmutated and/or mutated IgG1 mAbs in terms of pathogenic activity, we have precisely analyzed the roles of C1q-binding residues of the IgG1 Fc region (E318, K320, K322, P329, and P331) in initiating complement activation both in vitro and in vivo. These results are consistent with previous mutagenesis studies that showed that these binding residues are required for complement activation in vitro (22, 25, 27). The alanine substitution at these five single-residue sites variously decreased the CDC activity of the IgG1 mAb against hCOL17 NC16A. The IgG1 mAb that was mutated at P331 showed low CDC activity in vitro, and it failed to produce a BP phenotype in the COL17-humanized (*COL17*$^{m-/-,\ h+}$) mice. In contrast, the IgG1 mAbs mutated at K322 or at E318 K320 K322 showed moderate CDC activity in vitro and high (K322) to moderate (E318 K320 K322) pathogenic activity in vivo. The other mutated mAbs (E318A and K320A), which showed high CDC activity in vitro, showed high pathogenic activity in vivo. The results of in vivo pathogenic activity and in vitro CDC and ADCC activities are summarized in Supplemental Table III. The findings suggest that the moderate CDC activity of mutated mAbs is sufficient to induce skin detachment in neonatal COL17-humanized mice and that the P331 residue is the key residue for complement activation and is required for the pathogenic activity of IgG1 mAb in vivo. Thus, complement activation ability seems to correlate with the pathogenic effects of the mutated IgG1 mAbs in COL17-humanized mice (Fig. 5, Table III). Taken together, these findings further suggest that IgG1 Fc-dependent complement activation plays a major pathogenic role in subepidermal blister formation in BP.

In the classical complement pathway, C1q binding to IgG1 triggers proteolytic cascades, which result in the generation of a large amount of C3b. This explains why the immunofluorescence intensity of mouse C1q was weaker than that of mouse C3 in DIF examinations of mouse models, as shown in Fig. 8. In addition to C3b being capable of generating membrane attack complexes as the opsonin, it induces various inflammatory reactions by binding to the complement receptors expressed on the effector cells, such as granulocytes, monocytes, neutrophils, or mast cells (43–45). In our BP mouse model, inflammatory cells, such as mast cells, neutrophils, and lymphocytes, are observed at the dermis. It has been demonstrated that C3 binding to complement receptors stimulates activation and chemotaxis of neutrophils and/or mast cells (46). Mast cells can produce various mediators, such as leukotrienes, platelet-activating factor, and cytokines, that contribute directly or indirectly to neutrophil recruitment (47, 48). The neutrophils recruited into skin then releases elastase and gelatinase B, damaging the BMZ (49, 50). These data suggest that subepidermal blistering is mediated by a complement-dependent cellular (mast-cell and neutrophil) cytotoxicity pathway.

In addition to IgG1 Abs activating complement cascades, they may directly recruit and activate effector cells via the interaction between the Fc region and reciprocal FcγRs. In this study, we analyzed the Fc-FcγR–mediated ADCC activity of IgG1 mAbs. That activity was fully defective in the IgG1 mAb that was mutated at P329, and the mutation at P331 moderately reduced the activity of the IgG1 mAb (Fig. 6). In contrast, the other mutated mAbs (E318A, K320A, K322A, and E318A K320A K322A)

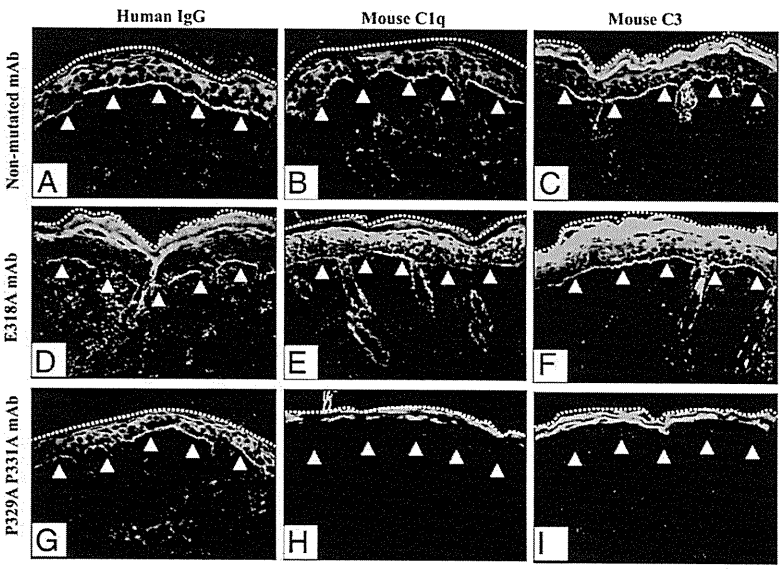

FIGURE 8. Capability of activating complement in vivo for the non-mutated and mutated IgG1 mAbs. In these three models (Fig. 7), 48 h after injection of the IgG1 mAbs, the complement activation capability was determined by DIF of human IgG and mouse complement components C1q and C3. All three of the mAbs (nonmutated IgG1, mutated E318A, and mutated P329A P331A) deposit at the DEJ (white arrowheads) (skin surface, white dotted line) of mouse skin (*A*, *D*, *G*). Mouse complement components C1q and C3 (green, FITC) are activated by the nonmutated (*B*, *C*) and E318A mAbs (*E*, *F*) but not by P329A P331A (*H*, *I*) at the DEJ (white arrowheads). Original magnification ×200 (*A–I*).

showed similar ADCC activity to that of the nonmutated IgG1 mAb. These results indicate that P329 is a key residue in IgG1-dependent ADCC reaction and that P331 plays a minor role in that process. A site-directed mutagenesis study also demonstrated that alanine substitution at the P329 residue causes the dual deficiencies of ADCC and CDC activity in vitro (25). If we focus on the pathogenic activity of IgG1 mAbs in BP, our mutagenesis studies suggest that Fc-FcγR–mediated ADCC activity may have contributed to the blister formation. In this study, in vitro CDC analysis showed that P329A and K322A had similarly moderate CDC activity (Fig. 5) but mutually distinct ADCC activity (Fig. 6). K322A showed normal ADCC activity, and P329A was incapable of triggering the ADCC reaction. Our in vivo results showed almost no skin detachment for the P329A-mutated mAb (one of seven mice) but some skin detachment for the K322A mAb (five of eight mice) (Table III). These results suggest that the ADCC (FcγR-dependent immune reaction) plays a minor but augmenting role in IgG1-dependent blister formation. This concept is further supported by a previous report by Mihai et al. (41) in which the pathogenicity of BP IgG1 and IgG4 autoantibodies was amplified by the additional recruitment of neutrophils and mast cells via Fc–FcγR interaction.

Recently, our group has used a phage display technique to develop a monoclonal Fab Ab against hCOL17 NC16A from BP patients (51). The monoclonal Fab Ab lacked pathogenic activity when administrated to neonatal COL17-humanized ($COL17^{m-/-,\ h+}$) mice. Furthermore, the monoclonal Fab Ab competitively protected the COL17-humanized ($COL17^{m-/-,\ h+}$) mice from the blister formation that would normally be induced by IgG autoantibodies prepared from BP patients. These results are consistent with our current study, and they further suggest the crucial role of the IgG1 Fc region in BP pathomechanism. In addition, complete IgG1 Ab has a longer half-life than Fab Ab in vivo (52, 53). Therefore, our current study raises the possibility that complete IgG1 mAbs with mutation at the C1q binding sites of the Fc region would protect the pathogenic epitopes from attack by the autoantibodies not only in BP but also in other autoimmune diseases in which complement activation plays an essential role.

In conclusion, to our knowledge, this study is the first in vivo evidence that IgG1 Abs targeting hCOL17 NC16A alone can trigger blister formation, and it suggests that IgG1-dependent complement activation via IgG1 Fc–C1q interaction plays a crucial role in BP.

Acknowledgments

We thank Drs. Yasuyuki Fujita, Yasuki Tateishi, and Daichi Hoshina (Hokkaido University Graduate School of Medicine) for kind discussion and technical assistance. We also thank Noriko Ikeda, Yui Kashima, Mika Tanabe, Yuko Hayakawa, and Akari Nagasaki (Hokkaido University Graduate School of Medicine) for technical assistance; Drs. Daisuke Inokuma (Hokkaido University Hospital, Sapporo), Yuka Oguchi, and Kazuo Kodama (JR Sapporo Hospital, Sapporo) for providing BP patient blood; and Dr. Kim B. Yancey for providing hCOL17 cDNA (University of Texas Southwestern Medical Center, Dallas, TX).

Disclosures

The authors have no financial conflicts of interest.

References

1. Gudi, V. S., M. I. White, N. Cruickshank, R. Herriot, S. L. Edwards, F. Nimmo, and A. D. Ormerod. 2005. Annual incidence and mortality of bullous pemphigoid in the Grampian Region of North-east Scotland. *Br. J. Dermatol.* 153: 424–427.
2. Langan, S. M., L. Smeeth, R. Hubbard, K. M. Fleming, C. J. Smith, and J. West. 2008. Bullous pemphigoid and pemphigus vulgaris—incidence and mortality in the UK: population based cohort study. *BMJ* 337: a180.
3. Jordon, R. E., E. H. Beutner, E. Witebsky, G. Blumental, W. L. Hale, and W. F. Lever. 1967. Basement zone antibodies in bullous pemphigoid. *J. Am. Med. Assoc.* 200: 751–756.
4. Nishie, W., D. Sawamura, K. Natsuga, S. Shinkuma, M. Goto, A. Shibaki, H. Ujiie, E. Olasz, K. B. Yancey, and H. Shimizu. 2009. A novel humanized neonatal autoimmune blistering skin disease model induced by maternally transferred antibodies. *J. Immunol.* 183: 4088–4093.
5. Bernard, P., P. Aucouturier, F. Denis, and J. M. Bonnetblanc. 1990. Immunoblot analysis of IgG subclasses of circulating antibodies in bullous pemphigoid. *Clin. Immunol. Immunopathol.* 54: 484–494.
6. Hofmann, S., S. Thoma-Uszynski, T. Hunziker, P. Bernard, C. Koebnick, A. Stauber, G. Schuler, L. Borradori, and M. Hertl. 2002. Severity and phenotype of bullous pemphigoid relate to autoantibody profile against the NH_2- and COOH-terminal regions of the BP180 ectodomain. *J. Invest. Dermatol.* 119: 1065–1073.
7. Laffitte, E., M. Skaria, F. Jaunin, K. Tamm, J. H. Saurat, B. Favre, and L. Borradori. 2001. Autoantibodies to the extracellular and intracellular domain of bullous pemphigoid 180, the putative key autoantigen in bullous pemphigoid, belong predominantly to the IgG1 and IgG4 subclasses. *Br. J. Dermatol.* 144: 760–768.
8. Stanley, J. R., P. Hawley-Nelson, S. H. Yuspa, E. M. Shevach, and S. I. Katz. 1981. Characterization of bullous pemphigoid antigen: a unique basement membrane protein of stratified squamous epithelia. *Cell* 24: 897–903.
9. Sitaru, C., E. Schmidt, S. Petermann, L. S. Munteanu, E. B. Bröcker, and D. Zillikens. 2002. Autoantibodies to bullous pemphigoid antigen 180 induce dermal-epidermal separation in cryosections of human skin. *J. Invest. Dermatol.* 118: 664–671.
10. Giudice, G. J., D. J. Emery, B. D. Zelickson, G. J. Anhalt, Z. Liu, and L. A. Diaz. 1993. Bullous pemphigoid and herpes gestationis autoantibodies recognize a common non-collagenous site on the BP180 ectodomain. *J. Immunol.* 151: 5742–5750.
11. Anhalt, G. J., C. F. Bahn, R. S. Labib, J. J. Voorhees, A. Sugar, and L. A. Diaz. 1981. Pathogenic effects of bullous pemphigoid autoantibodies on rabbit corneal epithelium. *J. Clin. Invest.* 68: 1097–1101.
12. Liu, Z., L. A. Diaz, J. L. Troy, A. F. Taylor, D. J. Emery, J. A. Fairley, and G. J. Giudice. 1993. A passive transfer model of the organ-specific autoimmune disease, bullous pemphigoid, using antibodies generated against the hemidesmosomal antigen, BP180. *J. Clin. Invest.* 92: 2480–2488.
13. Oikarinen, A. I., J. J. Zone, A. R. Ahmed, U. Kiistala, and J. Uitto. 1983. Demonstration of collagenase and elastase activities in the blister fluids from bullous skin diseases: comparison between dermatitis herpetiformis and bullous pemphigoid. *J. Invest. Dermatol.* 81: 261–266.
14. Ståhle-Bäckdahl, M., M. Inoue, G. J. Guidice, and W. C. Parks. 1994. 92-kD Gelatinase is produced by eosinophils at the site of blister formation in bullous pemphigoid and cleaves the extracellular domain of recombinant 180-kD bullous pemphigoid autoantigen. *J. Clin. Invest.* 93: 2022–2030.
15. Liu, Z., W. Sui, M. Zhao, Z. Li, N. Li, R. Thresher, G. J. Giudice, J. A. Fairley, C. Sitaru, D. Zillikens, et al. 2008. Subepidermal blistering induced by human autoantibodies to BP180 requires innate immune players in a humanized bullous pemphigoid mouse model. *J. Autoimmun.* 31: 331–338.
16. Chen, R., G. Ning, M. L. Zhao, M. G. Fleming, L. A. Diaz, Z. Werb, and Z. Liu. 2001. Mast cells play a key role in neutrophil recruitment in experimental bullous pemphigoid. *J. Clin. Invest.* 108: 1151–1158.
17. Nishie, W., D. Sawamura, M. Goto, K. Ito, A. Shibaki, J. R. McMillan, K. Sakai, H. Nakamura, E. Olasz, K. B. Yancey, et al. 2007. Humanization of autoantigen. *Nat. Med.* 13: 378–383.
18. Nelson, K. C., M. Zhao, P. R. Schroeder, N. Li, R. A. Wetsel, L. A. Diaz, and Z. Liu. 2006. Role of different pathways of the complement cascade in experimental bullous pemphigoid. *J. Clin. Invest.* 116: 2892–2900.
19. Jordon, R. E., S. Kawana, and K. A. Fritz. 1985. Immunopathologic mechanisms in pemphigus and bullous pemphigoid. *J. Invest. Dermatol.* 85(Suppl. 1)72s–78s.
20. Provost, T. T., and T. B. Tomasi, Jr. 1973. Evidence for complement activation via the alternate pathway in skin diseases. I. Herpes gestationis, systemic lupus erythematosus, and bullous pemphigoid. *J. Clin. Invest.* 52: 1779–1787.
21. Jordon, R. E., N. K. Day, W. M. Sams, Jr., and R. A. Good. 1973. The complement system in bullous pemphigoid. I. Complement and component levels in sera and blister fluids. *J. Clin. Invest.* 52: 1207–1214.
22. Duncan, A. R., and G. Winter. 1988. The binding site for C1q on IgG. *Nature* 332: 738–740.
23. Burton, D. R. 1985. Immunoglobulin G: functional sites. *Mol. Immunol.* 22: 161–206.
24. Oganesyan, V., C. Gao, L. Shirinian, H. Wu, and W. F. Dall'Acqua. 2008. Structural characterization of a human Fc fragment engineered for lack of effector functions. *Acta Crystallogr. D Biol. Crystallogr.* 64: 700–704.
25. Idusogie, E. E., L. G. Presta, H. Gazzano-Santoro, K. Totpal, P. Y. Wong, M. Ultsch, Y. G. Meng, and M. G. Mulkerrin. 2000. Mapping of the C1q binding site on rituxan, a chimeric antibody with a human IgG1 Fc. *J. Immunol.* 164: 4178–4184.
26. Tao, M. H., R. I. Smith, and S. L. Morrison. 1993. Structural features of human immunoglobulin G that determine isotype-specific differences in complement activation. *J. Exp. Med.* 178: 661–667.
27. Xu, Y., R. Oomen, and M. H. Klein. 1994. Residue at position 331 in the IgG1 and IgG4 C_H2 domains contributes to their differential ability to bind and activate complement. *J. Biol. Chem.* 269: 3469–3474.
28. Döpp, R., E. Schmidt, I. Chimanovitch, M. Leverkus, E. B. Bröcker, and D. Zillikens. 2000. IgG4 and IgE are the major immunoglobulins targeting the

NC16A domain of BP180 in *Bullous pemphigoid*: serum levels of these immunoglobulins reflect disease activity. *J. Am. Acad. Dermatol.* 42: 577–583.
29. Iwata, Y., K. Komura, M. Kodera, T. Usuda, Y. Yokoyama, T. Hara, E. Muroi, F. Ogawa, M. Takenaka, and S. Sato. 2008. Correlation of IgE autoantibody to BP180 with a severe form of bullous pemphigoid. *Arch. Dermatol.* 144: 41–48.
30. Amagai, M., A. Komai, T. Hashimoto, Y. Shirakata, K. Hashimoto, T. Yamada, Y. Kitajima, K. Ohya, H. Iwanami, and T. Nishikawa. 1999. Usefulness of enzyme-linked immunosorbent assay using recombinant desmogleins 1 and 3 for serodiagnosis of pemphigus. *Br. J. Dermatol.* 140: 351–357.
31. Amagai, M., K. Tsunoda, H. Suzuki, K. Nishifuji, S. Koyasu, and T. Nishikawa. 2000. Use of autoantigen-knockout mice in developing an active autoimmune disease model for pemphigus. *J. Clin. Invest.* 105: 625–631.
32. Ujiie, H., A. Shibaki, W. Nishie, D. Sawamura, G. Wang, Y. Tateishi, Q. Li, R. Moriuchi, H. Qiao, H. Nakamura, et al. 2010. A novel active mouse model for bullous pemphigoid targeting humanized pathogenic antigen. *J. Immunol.* 184: 2166–2174.
33. Kobayashi, M., M. Amagai, K. Kuroda-Kinoshita, T. Hashimoto, Y. Shirakata, K. Hashimoto, and T. Nishikawa. 2002. BP180 ELISA using bacterial recombinant NC16a protein as a diagnostic and monitoring tool for bullous pemphigoid. *J. Dermatol. Sci.* 30: 224–232.
34. Zillikens, D., P. A. Rose, S. D. Balding, Z. Liu, M. Olague-Marchan, L. A. Diaz, and G. J. Giudice. 1997. Tight clustering of extracellular BP180 epitopes recognized by bullous pemphigoid autoantibodies. *J. Invest. Dermatol.* 109: 573–579.
35. Galvin, J. E., M. E. Hemric, K. Ward, and M. W. Cunningham. 2000. Cytotoxic mAb from rheumatic carditis recognizes heart valves and laminin. *J. Clin. Invest.* 106: 217–224.
36. Traggiai, E., S. Becker, K. Subbarao, L. Kolesnikova, Y. Uematsu, M. R. Gismondo, B. R. Murphy, R. Rappuoli, and A. Lanzavecchia. 2004. An efficient method to make human monoclonal antibodies from memory B cells: potent neutralization of SARS coronavirus. *Nat. Med.* 10: 871–875.
37. Liang, M., S. Dübel, D. Li, I. Queitsch, W. Li, and E. K. Bautz. 2001. Baculovirus expression cassette vectors for rapid production of complete human IgG from phage display selected antibody fragments. *J. Immunol. Methods* 247: 119–130.
38. Poul, M. A., M. Cerutti, H. Chaabihi, M. Ticchioni, F. X. Deramoudt, A. Bernard, G. Devauchelle, M. Kaczorek, and M. P. Lefranc. 1995. Cassette baculovirus vectors for the production of chimeric, humanized, or human antibodies in insect cells. *Eur. J. Immunol.* 25: 2005–2009.
39. Liang, C. Y., H. Z. Wang, T. X. Li, Z. H. Hu, and X. W. Chen. 2004. High efficiency gene transfer into mammalian kidney cells using baculovirus vectors. *Arch. Virol.* 149: 51–60.
40. Schumaker, V. N., M. A. Calcott, H. L. Spiegelberg, and H. J. Müller-Eberhard. 1976. Ultracentifuge studies of the binding of IgG of different subclasses to the Clq subunit of the first component of complement. *Biochemistry* 15: 5175–5181.
41. Mihai, S., M. T. Chiriac, J. E. Herrero-González, M. Goodall, R. Jefferis, C. O. Savage, D. Zillikens, and C. Sitaru. 2007. IgG4 autoantibodies induce dermal-epidermal separation. *J. Cell. Mol. Med.* 11: 1117–1128.
42. Liu, Z., G. J. Giudice, S. J. Swartz, J. A. Fairley, G. O. Till, J. L. Troy, and L. A. Diaz. 1995. The role of complement in experimental bullous pemphigoid. *J. Clin. Invest.* 95: 1539–1544.
43. Ricklin, D., and J. D. Lambris. 2007. Complement-targeted therapeutics. *Nat. Biotechnol.* 25: 1265–1275.
44. Melamed, J., M. A. Arnaout, and H. R. Colten. 1982. Complement (C3b) interaction with the human granulocyte receptor: correlation of binding of fluid-phase radiolabeled ligand with histaminase release. *J. Immunol.* 128: 2313–2318.
45. Lambris, J. D., D. Ricklin, and B. V. Geisbrecht. 2008. Complement evasion by human pathogens. *Nat. Rev. Microbiol.* 6: 132–142.
46. Müller-Eberhard, H. J. 1988. Molecular organization and function of the complement system. *Annu. Rev. Biochem.* 57: 321–347.
47. Galli, S. J., J. R. Gordon, and B. K. Wershil. 1991. Cytokine production by mast cells and basophils. *Curr. Opin. Immunol.* 3: 865–872.
48. Galli, S. J. 1993. New concepts about the mast cell. *N. Engl. J. Med.* 328: 257–265.
49. Liu, Z., G. J. Giudice, X. Zhou, S. J. Swartz, J. L. Troy, J. A. Fairley, G. O. Till, and L. A. Diaz. 1997. A major role for neutrophils in experimental bullous pemphigoid. *J. Clin. Invest.* 100: 1256–1263.
50. Liu, Z., J. M. Shipley, T. H. Vu, X. Zhou, L. A. Diaz, Z. Werb, and R. M. Senior. 1998. Gelatinase B-deficient mice are resistant to experimental bullous pemphigoid. *J. Exp. Med.* 188: 475–482.
51. Wang, G., H. Ujiie, A. Shibaki, W. Nishie, Y. Tateishi, K. Kikuchi, Q. Li, J. R. McMillan, H. Morioka, D. Sawamura, et al. 2010. Blockade of autoantibody-initiated tissue damage by using recombinant fab antibody fragments against pathogenic autoantigen. *Am. J. Pathol.* 176: 914–925.
52. Holliger, P., and P. J. Hudson. 2005. Engineered antibody fragments and the rise of single domains. *Nat. Biotechnol.* 23: 1126–1136.
53. Kane, S. V., and L. A. Acquah. 2009. Placental transport of immunoglobulins: a clinical review for gastroenterologists who prescribe therapeutic monoclonal antibodies to women during conception and pregnancy. *Am. J. Gastroenterol.* 104: 228–233.

Correspondence

Two cases of cutaneous sporotrichosis in continental/microthermal climate zone: global warming alert?

doi: 10.1111/j.1365-2230.2010.03795.x

Sporotrichosis is commonly encountered in tropical and subtropical areas, but rarely in continental/microthermal climate zones as defined by the Köppen–Geiger Climate Classification.[1] We report two cases of cutaneous sporotrichosis in Hokkaido, an island in the continental/microthermal climate zone in Japan.

Patient 1 was a 55-year-old Japanese woman, who presented in 2009 with a 6-month history of two dark-red, crusted, infiltrated skin lesions measuring about 10 mm and 2 mm, respectively, on the left upper eyelid (Fig. 1a). She was working as a farmer in Hokkaido and had never lived in any other part of Japan. Histopathological examination of haematoxylin and eosin-stained specimens showed a prominent epidermal hyperplasia and abundant inflammatory infiltration in the dermis. Periodic-acid–Schiff (PAS) and Grocott's methenamine silver (GMS) stains revealed a few round and budding yeast-like cells scattered in the dermis, occasionally within a giant cell. Cultures of the tissue sections of lesion on Sabouraud dextrose agar and potato dextrose agar grew dark-brown velvety colonies. Slide cultures from the colonies contained septate branching hyphae, with slender, tapering conidiophores arising at right angles. A sporotrichin skin test gave a positive reaction.

Patient 2 was a 55-year-old man, who presented in 2002 with a chronic erosive nodule measuring 20 × 10 mm on the left mandible, which had been present for over 1 year on 2002 (Fig. 1b). He was working as a carpenter in Hokkaido, and had never lived in any other part of the country. Histopathological analysis found prominent epidermal hyperplasia and a chronic granulomatous inflammatory cell infiltrate. PAS and GMS stained round yeast-like cells scattered throughout the dermis. Cultures of the biopsied tissue samples grown on Sabouraud dextrose agar produced dark-brown velvety colonies. Slide cultures from the colonies contained septate, branching hyphae. Sporotrichin skin test gave a positive reaction.

Cutaneous sporotrichosis is a fungal infection commonly encountered in tropical and subtropical areas.[1] In Japan, > 3500 cases of cutaneous sporotrichosis were reported as of 2001 on Honshu Island, which falls in the temperate/mesothermal climate zone.[2] By contrast, no case reports were reported from Hokkaido in English journals before 2004. Similarly, few cases have been reported in other continental/microthermal climate zone around the world,[3] suggesting that cutaneous sporotrichosis is extremely rare in that zone. This geographical difference in reported cases may be due to the fact that *Sporothrix schenckii*, the pathogenic fungus that causes sporotrichosis, prefers moderate temperatures (around 22 °C).[1] The yearly temperature in Hokkaido

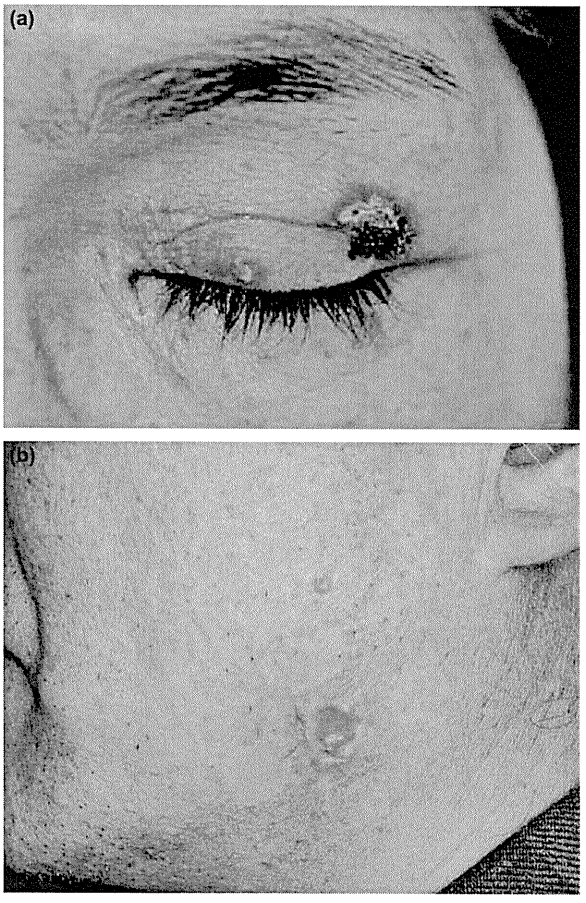

Figure 1 (a) Patient 1. Nodule and papule on the left upper eyelid. (b) Patient 2. Nodule on the left mandible.

averaged for the years 2000–2008 was 9.1 °C, so these results further suggest that *S. schenckii* rarely occurs in Hokkaido. Interestingly, three cases of cutaneous sporotrichosis, including our two, have been reported from Hokkaido in the Japanese literature since 2000, whereas only one case was recorded before 2000. We suggest that the prevalence of cutaneous sporotrichosis in Hokkaido may be increasing as a result of recent global warming.

Acknowledgement

We thank Dr H. I. Shibaki for technical assistance with the cultures.

D. Inokuma, A. Shibaki and H. Shimizu
Department of Dermatology, Hokkaido University Graduate School of Medicine, N15 W7, Sapporo 060-8638, Japan
E-mail: inokuma@med.hokudai.ac.jp
Conflict of interest: none declared.
Accepted for publication 7 December 2009

References

1 Bustamante B, Campos P. Endemic sporotrichosis. *Curr Opin Infect Dis* 2001; **14**: 145–9.
2 Kikuchi I, Morimoto K, Kawana S *et al.* Usefulness of itraconazole for sporotrichosis in Japan: study of three cases and literature comparison of therapeutic effects before and after release on the market. *Eur J Dermatol* 2006; **16**: 42–7.
3 Bargman H. Successful treatment of cutaneous sporotrichosis with liquid nitrogen: report of three cases. *Mycoses* 1995; **38**: 285–7.

The Fas/Fas ligand system, rather than granzyme B, may represent the main mediator of epidermal apoptosis in dermatomyositis

doi: 10.1111/j.1365-2230.2010.03808.x

We read with interest the paper by Grassi *et al.*[1] reporting an immunohistochemical study on cutaneous lesions of lupus erythematosus (CLE) and dermatomyositis (DM). A particularly interesting finding was that the expression of granzyme B (GrB), a pro-apoptotic serine-protease, was higher in CLE rthan in DM lesions. As GrB is mainly expressed by CD8+ lymphocytes, we were puzzled to read that 'in DM, the CD8+ subpopulation represented > 50% of the lymphocytic population'.[1] This finding is in striking contrast to a study in which our research group found that the CD4/CD8 ratio is approximately 2.5 in DM skin lesions.[2] On the other hand, the number of infiltrating CD8+ cells was reported to be similar to that of the CD4+ cells in CLE in both papers.[1,2] As previous studies also reported a similar level of apoptotic phenomena in lesional epidermis in both CLE and DM,[3,4] it is evident that GrB is not likely to represent a major mechanism of cell death in DM lesions.

We report the results from an ongoing study on skin lesions of six patients with DM, five patients with subacute CLE (SCLE) and five patients with discoid CLE (DLE). The sun-protected, clinically healthy skin of the patients served as internal controls, and five healthy donors comprised the control group. Immunohistochemical examination, performed as described previously,[2] included antibodies to Bax, a pro-apoptotic molecule involved in the mitochondrial pathway of apoptosis and activated by GrB; Bcl-2, its antiapoptotic counterpart also belonging to the mitochondrial pathway; Fas and Fas ligand (Fas-L), two key molecules triggering the death receptor pathway of apoptosis; and caspase 3, the final effector of both pathways. The following monoclonal antibodies were used. Bax: 1 : 500 dilution, clone YTH-2D2 (R&D Systems, MN, USA); Bcl-2: 1 : 1000 dilution, clone 124 (Dako, Copenhagen, Denmark); Fas: 1 : 60 dilution, clone GM30 (Novocastra Laboratories Ltd., Newcastle upon Tyne, UK); FasL): 1 : 50 dilution, clone 5D1 (Novocastra); caspase 3: 1 : 50 dilution, clone 5A1 (Cell Signaling, Danvers, MA, USA).

There was higher expression of Bax than of Bcl-2 in patient epidermis (Table 1). Fas was strongly expressed in epidermal sections from patients with DM (Fig. 1a) and CLE, and there was focal positivity in the healthy skin of these patients. Caspase 3 was expressed strongly in all lesional specimens and moderately in the healthy skin of patients.

Table 1 Semiquantitative evaluation of apoptotic molecules in lesional sections and controls.

	DM	DM-HS	SCLE	SCLE-HS	DLE	DLE-HS	HC
Bax	++	++	+++	++	+++	+	+
Bcl-2	+	+	+	+	++	+	+
Fas	+++	+	+++	+	+++	+	–
FasL	++	+	+++	+	++	+	–
Caspase 3	+++	++	+++	++	+++	++	+

DM, lesional epidermis of dermatomyositis; DM-HS, epidermis of sunprotected healthy skin from patients with DM; SCLE, lesional epidermis of subacute cutaneous lupus erythematosus; SCLE-HS, epidermis of sunprotected healthy skin from patients with SCLE; DLE, lesional epidermis of discoid cutaneous lupus erythematosus; DLE-HS, epidermis of sunprotected healthy skin from patients with DLE; HC, epidermis of sunprotected healthy skin from healthy controls. Semiquantitative evaluation of epidermal positivity for Bax, Bcl-2, Fas and caspase 3: –, negative; +, focal; ++, continuous basal; +++, basal and suprabasal. Semiquantitative evaluation of dermal positivity for FasL: –, negative; +, 0–5 cells; ++, 6–10 cells and +++, > 10 cells).

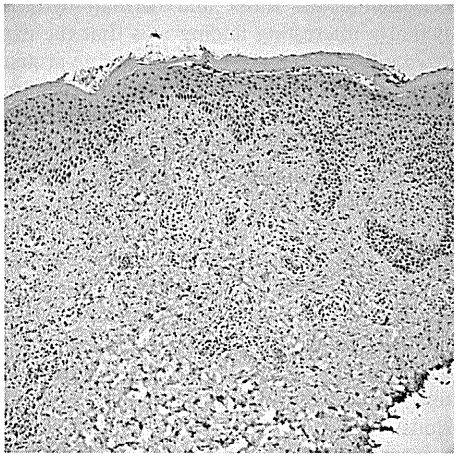

Fig 2. Immunohistochemistry of skin for angiopoietin-2. Note the abundant staining in the basal epidermis and dermal inflammatory cells. (Original magnification: ×100.)

National Institutes of Health, and a Veterans Administration Hospital Merit Award (to J.L.A.)

Conflicts of interest: None declared.

Reprint requests: Jack L. Arbiser, MD, PhD, Department of Dermatology, Emory University School of Medicine, WMB 5309, 1639 Pierce Dr, Atlanta, GA 30322.

E-mail: jarbise@emory.edu

REFERENCES

1. Bhandarkar SS, MacKelfresh J, Fried L, Arbiser JL. Targeted therapy of oral hairy leukoplakia with gentian violet. J Am Acad Dermatol 2008;58:711-2.
2. Lambeth JD, Kawahara T, Diebold B. Regulation of Nox and Duox enzymatic activity and expression. Free Radic Biol Med 2007;43:319-31.
3. Perry BN, Govindarajan B, Bhandarkar SS, Knaus UG, Valo M, Sturk C, et al. Pharmacologic blockade of angiopoietin-2 is efficacious against model hemangiomas in mice. J Invest Dermatol 2006;126:2316-22.
4. Brockow K, Grabenhorst P, Abeck D, Traupe B, Ring J, Hoppe U, et al. Effect of gentian violet, corticosteroid and tar preparations in *Staphylococcus aureus*—colonized atopic eczema. Dermatology 1999;199:231-6.
5. Howell MD, Novak N, Bieber T, Pastore S, Girolomoni G, Boguniewicz M, et al. Interleukin-10 downregulates anti-microbial peptide expression in atopic dermatitis. J Invest Dermatol 2005;125:738-45.

doi:10.1016/j.jaad.2009.05.027

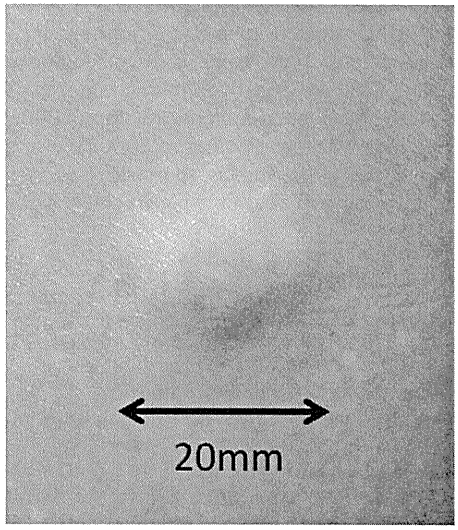

Fig 1. A slightly violaceous nodule on the middle aspect of the left thigh.

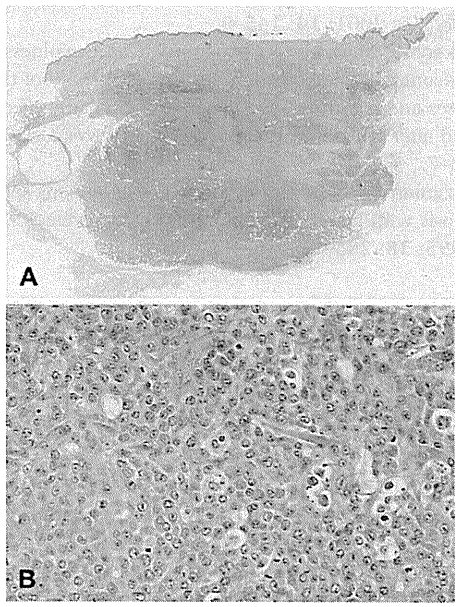

Fig 2. Skin biopsy findings. **A**, Dense, nodular, diffuse infiltrate of monotonous uniform cells involving the dermis and subcutaneous fat. **B**, A nodule of cells with round nuclei; prominent single or multiple nucleoli; abundant pale, slightly eosinophilic cytoplasm; and a number of atypical mitotic figures.

Aleukemic leukemia cutis with extensive bone involvement

To the Editor: Aleukemic leukemia cutis (ALC) is a rare condition that is characterized by the invasion of leukemic cells into the skin before such cells are observed in the peripheral blood.[1] We present a case of ALC with multiple bone metastases.

An 81-year-old man had a 2-month history of asymptomatic nodules on his trunk and legs. The physical examination revealed five subcutaneous nodules measuring up to 10 mm in size on his back and legs and a firm, slightly violaceous nodule